Spring 5-31-2013

Engineering spores to display g protein-coupled receptors for directed evolution

Alyssa Misoo Kim
New Jersey Institute of Technology

Copyright Warning & Restrictions

The copyright law of the United States (Title 17, United States Code) governs the making of photocopies or other reproductions of copyrighted material.

Under certain conditions specified in the law, libraries and archives are authorized to furnish a photocopy or other reproduction. One of these specified conditions is that the photocopy or reproduction is not to be "used for any purpose other than private study, scholarship, or research." If a, user makes a request for, or later uses, a photocopy or reproduction for purposes in excess of "fair use" that user may be liable for copyright infringement,

This institution reserves the right to refuse to accept a copying order if, in its judgment, fulfillment of the order would involve violation of copyright law.

Please Note: The author retains the copyright while the New Jersey Institute of Technology reserves the right to distribute this thesis or dissertation

Printing note: If you do not wish to print this page, then select "Pages from: first page # to: last page #" on the print dialog screen

ABSTRACT

ENGINEERING SPORES TO DISPLAY G PROTEIN-COUPLED RECEPTORS FOR DIRECTED EVOLUTION

by
Alyssa Misoo Kim

All human cells are surrounded by a plasma membrane made from a phospholipid bilayer, which is responsible for maintaining a biologically active species, while stopping entry of deleterious substances from the outside. G protein-coupled receptors (GPCRs) are the membrane proteins, which transmit signals across the cell membrane. GPCRs are involved in almost every physiological process, and irregular control leads to pathological conditions. Therefore, they are major drug targets. Crystal structure determination is required to understand the molecular details of activation/deactivation. However, GPCRs are difficult to crystallize because of stability issues. An efficient protein engineering system needs to be developed. The goal is to design and create a system to display a heterologous protein on the *Bacillus subtilis* spore coat. Human parathyroid hormone receptor (huPTH1R) is used as a model system. HuPTH1R is a GPCR, which is vital in regulating calcium and phosphate levels in the blood.

Molecular biology is used to create the plasmid pDG1730 huPTH1R-CotC that fused huPTH1R to a spore coat protein, CotC. The plasmid is transformed into *B. subtilis*, and huPTH1R is successfully integrated into *B. subtilis* genome via recombination. This work represents the first system for GPCR display on the spore coat. Spore display overcomes many of the hurdles found in "traditional" protein display systems. Finally, this system can be used as a general method for engineering and optimizing membrane proteins by directed evolution.

ENGINEERING SPORES TO DISPLAY G PROTEIN-COUPLED RECEPTORS FOR DIRECTED EVOLUTION

by
Alyssa Misoo Kim

A Thesis
Submitted to the Faculty of
New Jersey Institute of Technology
in Partial Fulfillment of the Requirements for the Degree of
Master of Science in Pharmaceutical Engineering

Otto H. York Department of
Chemical, Biological and Pharmaceutical Engineering

May 2013

APPROVAL PAGE

ENGINEERING SPORES TO DISPLAY G PROTEIN-COUPLED RECEPTORS FOR DIRECTED EVOLUTION

Alyssa Misoo Kim

Dr. Edgardo T. Farinas, Thesis Co-advisor Date
Associate Professor and Chair of Chemistry and Environmental Science, NJIT

Dr. Piero M. Armenante, Thesis Co-advisor Date
Distinguished Professor of Chemical, Biological and Pharmaceutical Engineering, NJIT

Dr. Laurent Simon, Committee Member Date
Associate Professor of Chemical, Biological and Pharmaceutical Engineering, NJIT

BIOGRAPHICAL SKETCH

Author: Alyssa Misoo Kim

Degree: Master of Science

Date: May 2013

Undergraduate and Graduate Education:

- Master of Science in Pharmaceutical Engineering,
  New Jersey Institute of Technology, Newark, NJ, 2013

- Bachelor of Science in Biology,
  Kyung Hee University, Seoul, South Korea, 2008

Major: Pharmaceutical Engineering

Presentations:

Kim, A. M., Farinas, E. T., "Engineering Spores to Display G Protein-Coupled Receptors for Directed Evolution," ISPE New Jersey Chapter Student Poster Competition, New Brunswick, NJ, April, 2013.

This thesis is dedicated to my Mom and Dad, who taught me the value of education and my Sisters for support throughout my studies.

우리 사랑하는 가족, 김청균, 김봉이, 김미나, 김미연.
그동안 편안하게 언제나 옆에서 격려해주고 조언해주면서 끝까지 공부 잘 마칠 수 있게 도와주신거 너무 감사합니다.

ACKNOWLEDGMENT

I want to express my sincerest gratitude for my advisor, Dr. Edgardo T. Farinas for his guidance, support, and patience. Without his constant motivation completion of this work was not possible.

I am grateful Dr. Piero M. Armenante as a co-advisor and Dr. Laurent Simon as the member of thesis committee for their comments and suggestion.

I want to thank Otto H. York Department of Chemical, Biological and Pharmaceutical Engineering and Department of Chemistry and Environmental Science for assisting me with all the administrative procedures. I am also grateful to Office of Graduate Studies for providing financial assistance.

Finally, I want to thank National Institute of General Medical Sciences (NIGMS) in National Institutes of Health (NIH) and National Science Foundation (NSF) for providing funds for this research.

TABLE OF CONTENTS

TABLE OF CONTENTS
(Continued)

Chapter **Page**

LIST OF FIGURES

LIST OF FIGURES
(Continued)

LIST OF FIGURES
(Continued)

Figure **Page**

CHAPTER 1

INTRODUCTION

1.1 G Protein-Coupled Receptors

G protein-coupled receptors (GPCRs) are integral membrane proteins characterized by seven transmembrane helices (TM) connected by three extracellular loops (ECLs) and three intracellular loops (ICLs) [1, 2] (Figure. 1.1).

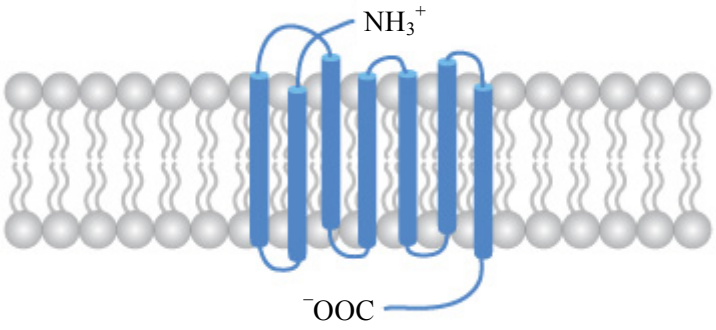

Figure 1.1 General structure of G protein-coupled receptors embedded in a lipid bilayer.

They are the largest family of membrane proteins in the human genome and function as the receptors for hormones, neurotransmitters, protons, ions, light, odors and gustative molecules [2]. Thus, they are essential for communication between internal and external environments of cells. For example, the human β_2 adrenergic receptor binds to adrenalin and noradrenalin on the exterior of the cell, and it leads to activate stimulation and regulation of the sympathetic nervous system.

GPCRs are involved in almost every physiological process. Hence, irregular control leads to pathological conditions, which include cancer, cardiovascular, metabolic, central nervous system and infectious diseases [1]. As a result, GPCRs are major human

drug targets. There are approximately 80 GPCR-targeting drugs in the current pharmaceutical market with annual sales reaching up to $50 billion, and they make approximately 30-50% of the drug targets [1]. Notable examples are Eli Lilly's Zyprexa (schizophrenia), Schering-Plough's Clarinex (hay fever and allergy symptoms), GlaxoSmithKline's Zantac (gastroesophageal reflux disease), and Novartis's Zelnorm (irritable bowel syndrome). Therefore, crystal structure determination would provide molecular details of activation and deactivation, which would have an enormous impact in drug discovery.

GPCRs are divided into five families based on their sequence and structural similarity: rhodopsin (Class A or Family 1), secretin/adhesion (Class B or Family 2), glutamate (Class C or Family 3), Frizzled and Taste2 [1-3]. The rhodopsin family is the largest and most diverse family among these families. There are four subfamilies in this diverse family: α, β, γ, δ. The α subfamily receptors activate the protons in retinal to detect the light. The β subfamily receptors, which include endothelin, gonadotropin-releasing hormone and oxytocin receptor ligands, bind to peptides. The γ subfamily consists of peptides or lipid-like receptors. Examples include somatostatin receptor 2 and 5, angiotensin receptor 1, and chemokine receptors, which are drug targets in this group. The δ subfamily is responsible for olfactory. The secretin family receptors bind peptide hormones like calcitonin, glucagon and parathyroid hormone. These hormones are used to regulate hypercalcaemia, hypoglycaemia and osteoporosis. In the glutamate family, there are four kinds of receptors that include metabotropic glutamate, $GABA_B$, sweet and umami taste, and calcium sensing. These three main families can be easily identified according by sequences comparison. Frizzled family consists of frizzled

and smoothened receptors involved in embrogenesis. The frizzled receptors bind Wnt glycoproteins, whereas smoothened receptors perform as the signaling unit. Last, Taste2 family consists of taste receptors including bitter sensing.

1.2 Crystal Structure and Problems

To date, there are only eight different crystal structures for GPCRs, which include rhodopsin [4, 5], β_2AR [6], β_1AR [7], adenosine A_{2A} receptor (ADORA2A) [8], histamine H_1 [9], sphingosine 1-phosphate [10], and CXCR4 chemokine receptor [11]. Despite huge research efforts in GPCR crystallography, determination of GPCRs structure is difficult due to the protein properties.

A protein needs to be functionally expressed, purified, and crystallized in order to successfully solve the crystal structure. However, there are several problems to determine the crystal structure of GPCRs. First, GPCR expression in native tissue is typically very low [12]; therefore, GPCRs need a recombinant expression system. GPCRs can be overexpress in prokaryotic system such as *Escherichia coli*. However, they are expressed as insoluble inclusion bodies. As a result, they must be solubilized and refolded using detergents and other chemical additives. Next, compared to soluble or cytoplasmic proteins, membrane proteins are difficult to crystallize because they are found in a lipid bilayer. This environment is difficult to mimic during the crystallization procedure. In the early 1980s, detergent-based micelles were designed to solubilize membrane proteins. In addition, bilayer vesicles, lipidic mesophase approaches, and lipid/detergent procedures were used to assist crystallization. Finally, GPCRs typically have thermodynamic and proteolytic protein stability problems [12]. As a result, there is a lack of secondary structure due to flexible segments of the protein.

The first GPCR structure was bovine rhodopsin (Figure. 1.2). This crystal structure has provided useful information for activation mechanism of GPCRs. Rhodopsin was more suitable for structural studies than most of other GPCRs because it can be obtained large quantities of functional protein from retinas, and they are thermally stable compared to other GPCRs.

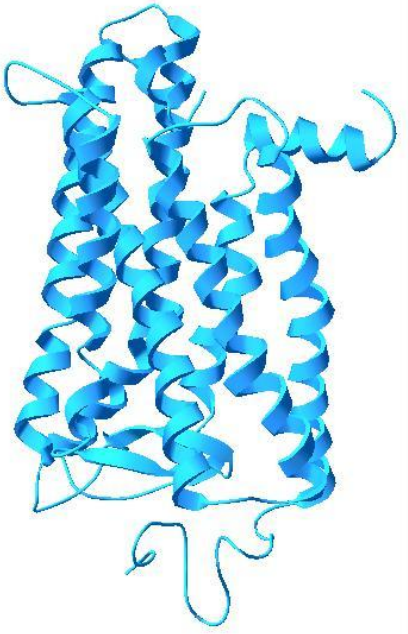

Figure 1.2 Structure of rhodopsin (PDB ID: 3PQR) [13].

In order to improve proteolytic stability, several protein engineering efforts have been employed. Recently, crystal structures of the human β_2 adrenocepter (β_2AR) as a receptor for adrenalin and noradrenalin have been determined. β_2AR was the first non-rhodopsin GPCR to be cloned and was one of the most extensively studied members. Two different protein engineering strategies were utilized. First, β_2AR was stabilized by binding a stable antibody fragment (Fab5) to the unstructured cytoplasmic ends of TM5 and TM6, which is linked by the third intracellular loop (ICL3) [14] (Figure. 1.3). Next,

the unstructured ICL3 sequence from Q230 to S262 was replaced with structured protein, T4 lysozyme (T4L) [14] (Figure. 1.4). In essence, a stable protein (antibody or lysozyme) was associated with the unstable GPCRs to impact an overall stable structure. In addition, β_1AR and β_2AR were further stabilized by addition of stabilizing ligands, amino acid substitutions, adding lipids, and high salt concentrations.

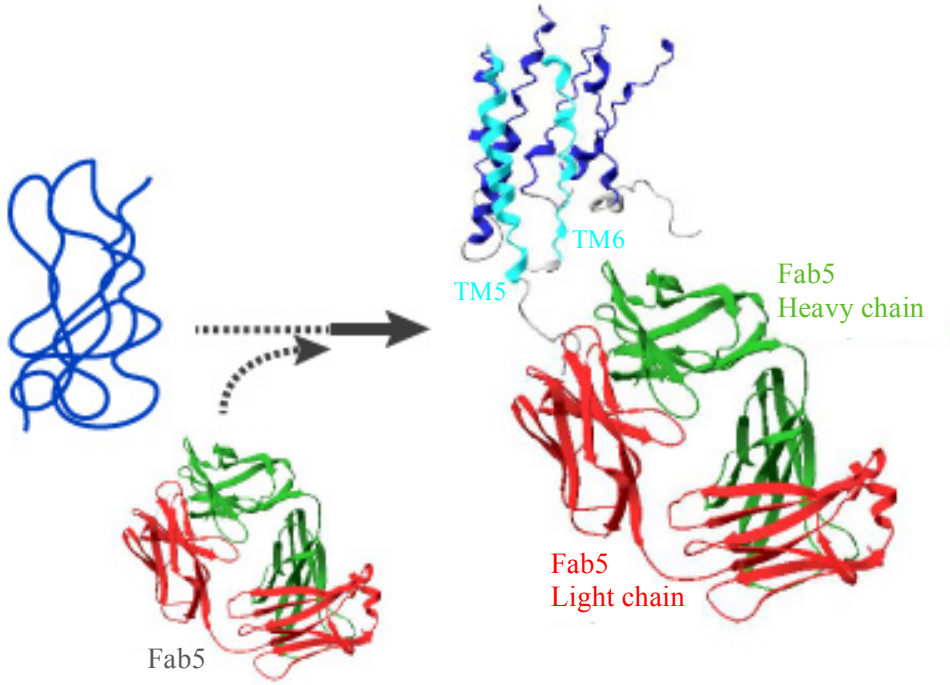

Figure 1.3 Structure of β_2AR-Fab5 (PDB ID: 2R4R) [6, 14].

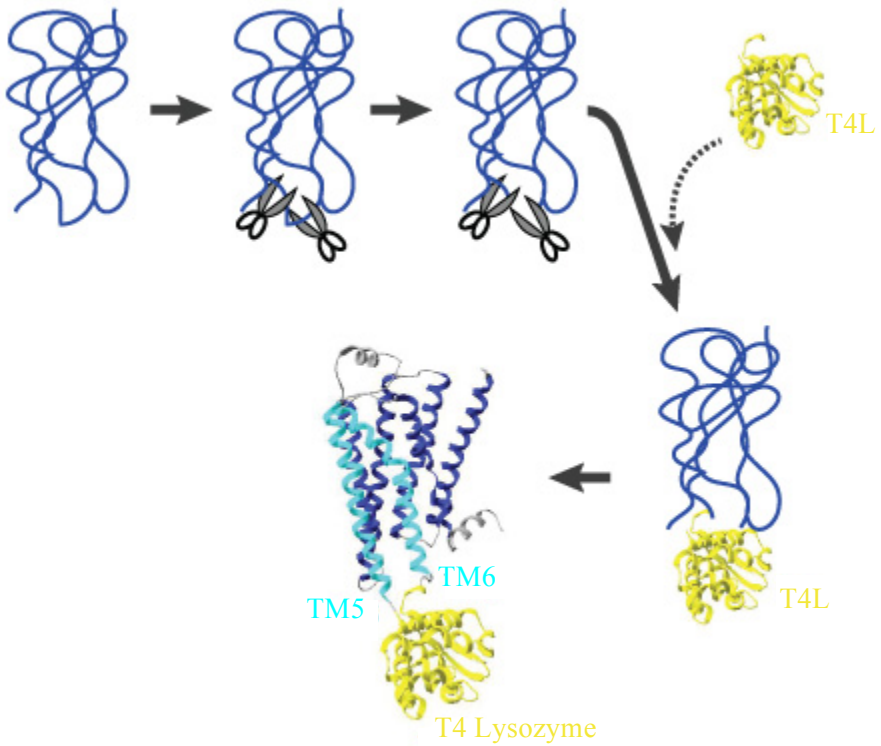

Figure 1.4 Structure of β_2AR-T4 lysozyme fusion [14] (PDB ID of β_2AR-T4 lysozyme: 2RH1[15] and T4 lysozyme: 206L[16]).

There are still no crystal structures for most of the rhodopsin family and other GPCR families such as the gamma-aminobutyric acid (GABA) or the metabotropic glutamate receptors (mGluRs) in family 3.

1.3 Directed Evolution

Darwinists believe the diversity found on Earth is due to evolution [17]. Evolution does not go toward a specific objective. It moves by random changes and it alters the capacity of an organism to reproduce under the present conditions. An adapted organism to the current conditions may fair better or worst when the environment changes. Next,

evolution requires a bit of “sloppiness”. This allows an organism to adapt to unexpected changes in the environment. Furthermore, evolution is based on the past. New structures and metabolic functions are created from pre-existing elements. Finally, evolution does not end, and does not go towards absolute complexity. We hold that human beings are at the top of the evolutionary scheme. However, a quick scan of the diversity of organisms shows that simpler ones have not been extinct or stopped evolving. The timescale of months to years can occur for natural evolution. One example is the appearance of antibiotic resistant bacteria and enzymes that degrade chemically synthesized compounds *(18, 19)*.

The products of evolution occur on many different levels. It is responsible for the diversity of life. In addition, evolution can be seen all the way down to single molecules such as proteins. For example, human ribonuclease and angiogenin share similar tertiary structures (Figure. 1.5). However, they have completely different functions. Ribonuclease is a digestive enzyme while angiogenin stimulates blood vessel growth.

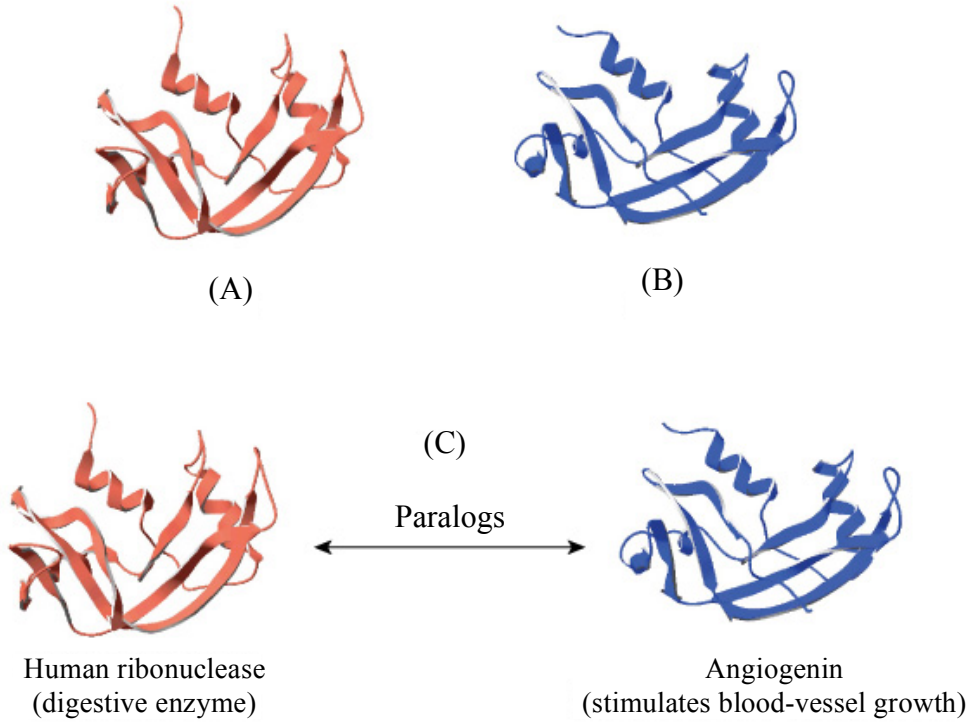

Figure 1.5 **(A)** Human ribonuclease (PDB ID: 5RSA) [(20)]. **(B)** Angiogenin (PDB ID: 1B1I) [(21)]. **(C)** Paralogs that perform different functions in one organism.

Protein engineering strategies can be roughly categorized as rational or evolutionary. Rational design requires detailed information of the protein structure and function. Guided by the structure, individual amino acids are chosen for substitution in order to modify the function. This is usually done by site directed mutagenesis [(22)]. Site directed mutagenesis is a molecular biology method. A specific nucleotide in the DNA is mutated, which results in change in an amino acid. Some successes include increased thermostability [(23-26)], altered substrate specificity [(27)], and introducing post translation modification [(28)]. The main disadvantage of rational design is the effect of the amino acid substitution cannot be predicted accurately. This is because we are still very ignorant on

how the changes affect every aspect of the protein. For example, we may be able to introduce a new function, such as altered substrate specificity. However, it is impossible to forecast the cost that the substitution has on a different property, such as thermostability. In conclusion, we need a huge amount of structural, mechanistic, and dynamic knowledge for a successful rational design effort. This information is only known for a small fraction of proteins.

On the other hand, directed evolution is a method that mimics the process of natural evolution in order to create mutants with novel and desired properties. The greatest advantage is that a detailed knowledge of structure or mechanism is not required. Directed evolution experiment has iterative cycles (Figure. 1.6). First, a library of genes up to 10^{15} members is generated by molecular biology techniques. Second, the DNA library is introduced into a suitable host. Typically, a library has 10^4-10^9 variants of the parent. Third, proteins from the library with improved functions are identified by appropriate screening or selection methods. Finally, the genes are used as parents for the next round of directed evolution. Through these repeated cycles, useful and desired mutations can accumulate like the natural evolution process. To name a few examples, directed evolution has been used to alter substrate specificity, increase thermal stability, organic solvent resistance, and enantioselectivity *(29-31)*.

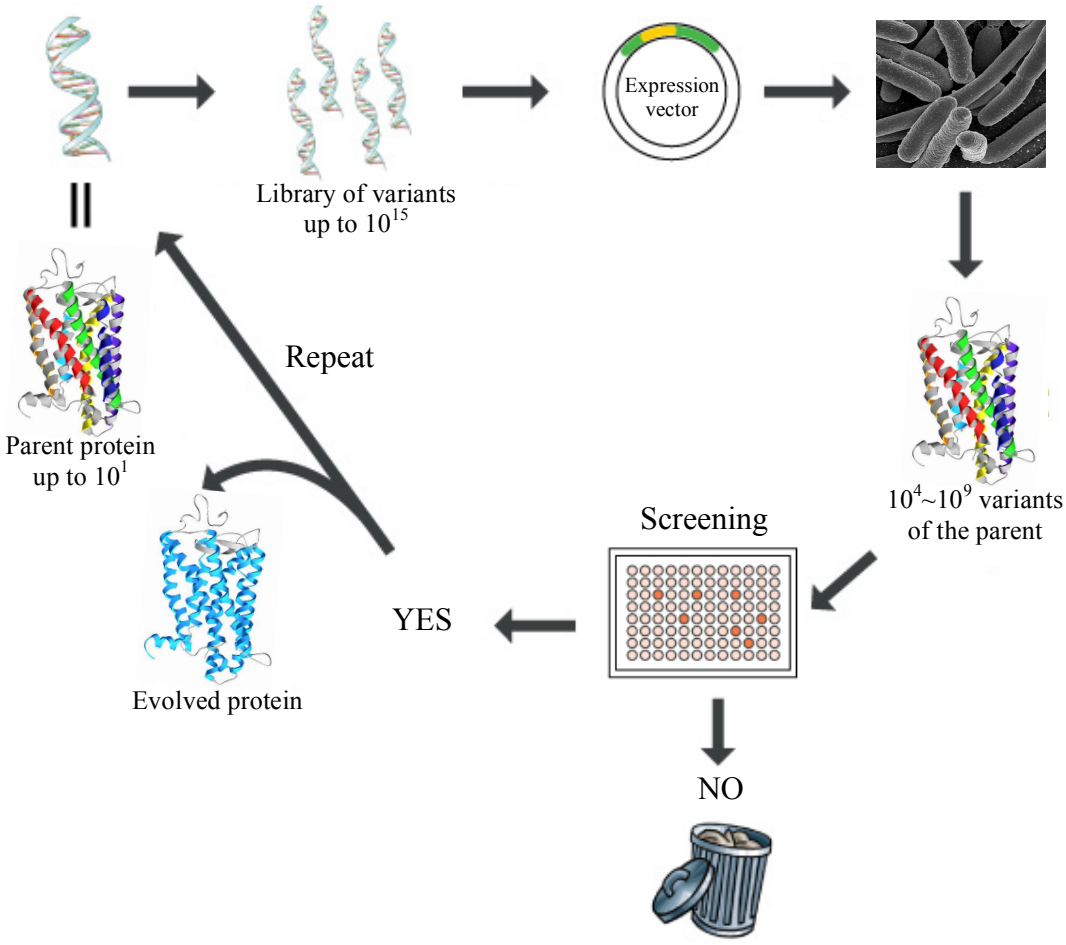

Figure 1.6 Basic steps of a directed evolution experiment. First, a library of genes is created. The library of variants is up to 10^{15}. Next, the library is cloned in an expression vector and transformed in a host cell. The desired proteins are screened or selected from the library. Finally, the improved proteins are used as parents for next round of evolution. (PDB ID: 3PQR) [13]

There are several techniques used to create libraries. As an example, the most common and successful methods are random mutagenesis, cassette mutagenesis, and *in vitro* gene recombination [32].

1.4 Protein Display

In nature, proteins localized on the cell surface are important to function. For example, they perform fundamental biological functions, including transportation such as importing and exporting molecules, adhesion molecules and receptors, communication between cells, signal transduction, and others [33]. Now, molecular biology has made it possible to use these cell surface proteins for biotechnological application. For example, microbial cell-surface display can be used to express a heterologous protein of interest as a fusion with various anchoring motifs as carrier proteins. Applications include peptide library screening [34-36], directed evolution of proteins [34, 35], vaccines development and targeted therapies [36-38], biocatalyst [36, 39], bioadsorption [36], mutation detection [36], biosensors [36], and bioremediation [34].

"Traditional" microorganisms used for protein display are phage [40], prokaryotes [33], and yeast [34, 41]. Protein display has several advantages when compared to libraries expressed in the cytoplasm (Figure. 1.7). For libraries expressed in the cytoplasm, a microtiter plate procedure may be needed to assay protein function. In a typical round of evolution, up to 10^3-10^4 protein variants can be conveniently assayed. Cells are usually arrayed in microtiter plates and they must be lysed to gain access to the protein. In this step, the genotype/phenotype connection is disconnected. Next, the cell debris may be required to be separated from the lysate. This step oftentimes necessitates multiple centrifugation and pipetting steps, which needs automated robotic systems. Furthermore, the lysate is a complex solution containing the target protein and the contents of the cytoplasm, which includes endogenous proteins, nucleic acids, etc.

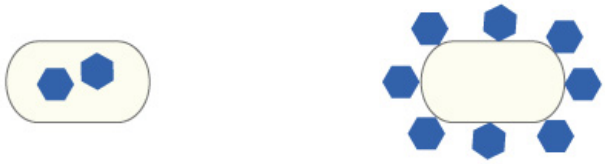

(A) (B)

Figure 1.7 **(A)** Proteins (Blue) which are expressed inside the host cell. **(B)** Proteins (Blue) which are displayed outside the host cell.

Protein display can overcome the obstacles presented above. First, the protein is freely accessible and assayed easily. Next, multiple liquid handling steps are not necessary because the cells are not lysed. Furthermore, the environment for screening such as pH, buffer composition, and ionic strength can be easily controlled. Finally, the genotype/phenotype remains intact.

A directed evolution strategy begins with determination of a suitable surface display platform (phage, prokaryote or yeast), based on characteristics of the protein. Gene libraries of the protein are created by random mutagenesis and/or recombination. Cloned genes are inserted into plasmid. They are transformed into a host and induced. Each cell has an individual member of the library on the cell surface, and screened for function. Next, the cells are cultured, the gene is isolated, and another round of evolution can be done (Figure. 1.8).

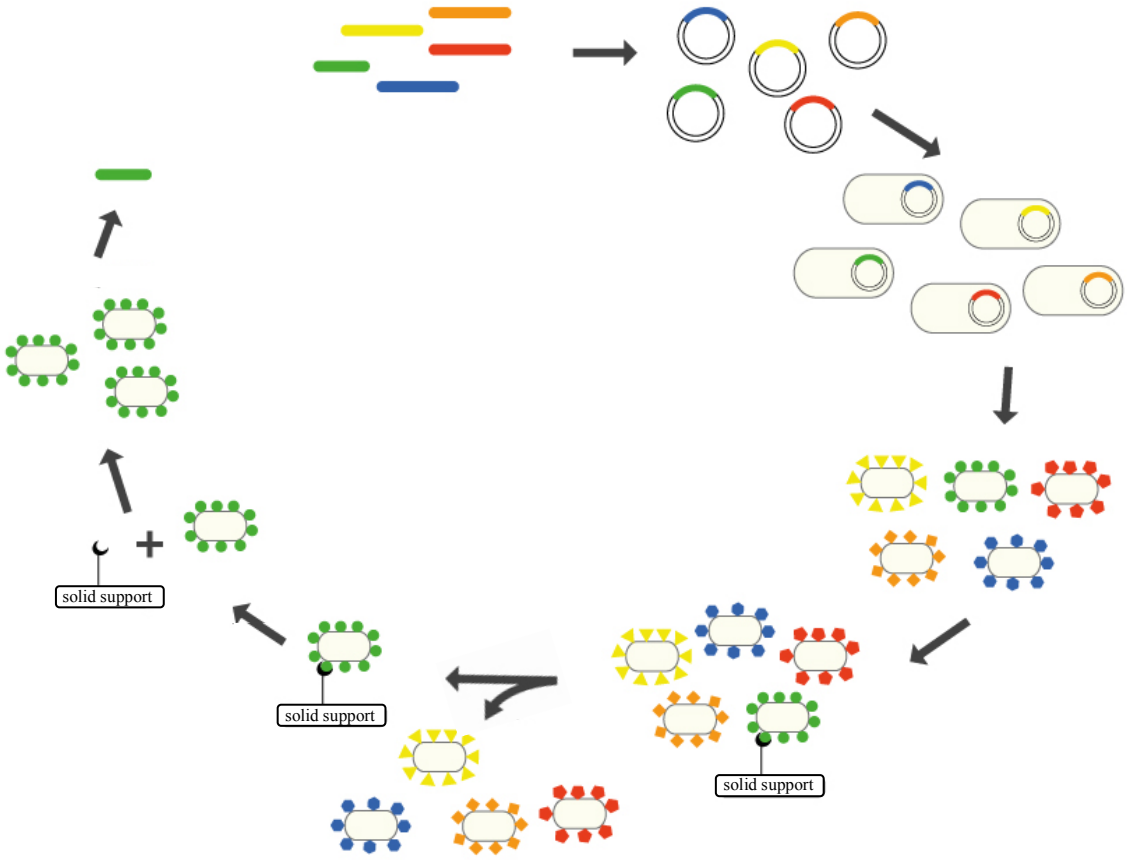

Figure 1.8 Protein screening of mutant libraries displayed the cell surface.

1.4.1 Phage Display

Bacteriophage is a virus that infects bacteria. Filamentous phage display was the first system, which was developed by George P. Smith, and it remains the most common. A peptide of interest can be fused with the pIII protein (Figure. 1.9) [42, 43]. T4 [39, 44, 45], T7 [39, 44], and λ phage [39, 44, 46] have also been used. Phage display has been used engineer antibodies [47, 48], discovery drug-like molecules [49], and molecular biomimetics [50]. In addition, they have been used for the protein engineering [51, 52].

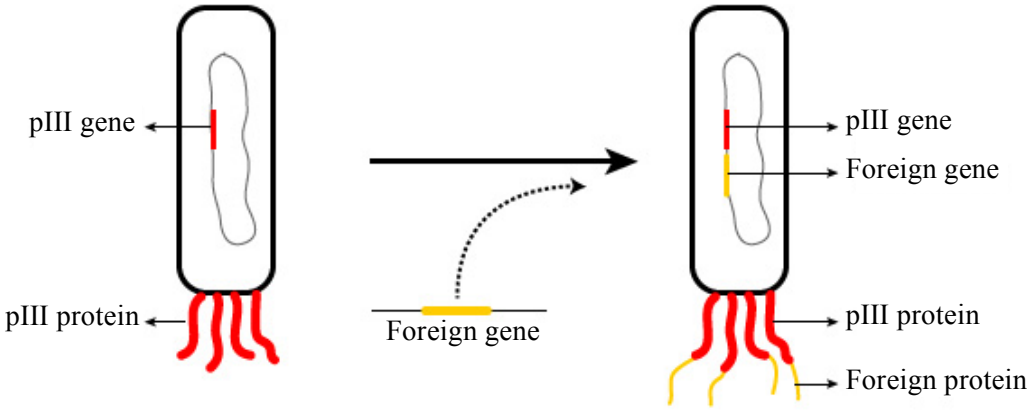

Figure 1.9 Phage display. A foreign protein of interest is fused with the pIII protein.

An advantage of phage display is that it is easy to perform and inexpensive. A library size of 10^{10} can be screened in a single day. Usually, three to five cycles are enough to generate peptide sequences with high binding efficiency. However, the size of the foreign protein to be displayed on the surface of phage is rather limited.

1.4.2 Microbial Cell Surface Display

Functional enzymes, peptides libraries, and antibody fragments have been displayed on the cell surfaces of bacteria [(34)]. There are two microbial cell surface display systems, gram-negative and positive. First, the architecture of gram-negative bacteria membrane includes an inner membrane and outer membrane, and sandwiched between the two is a peptidoglycan structure. Outer membrane proteins have been used as carriers to display foreign proteins on the surface (Figure. 1.10). Foreign genes can be fused to outer membrane proteins such as OmpA and the OmpC, PhoE, LamB, FhuA, and BtuB [(33, 53)].

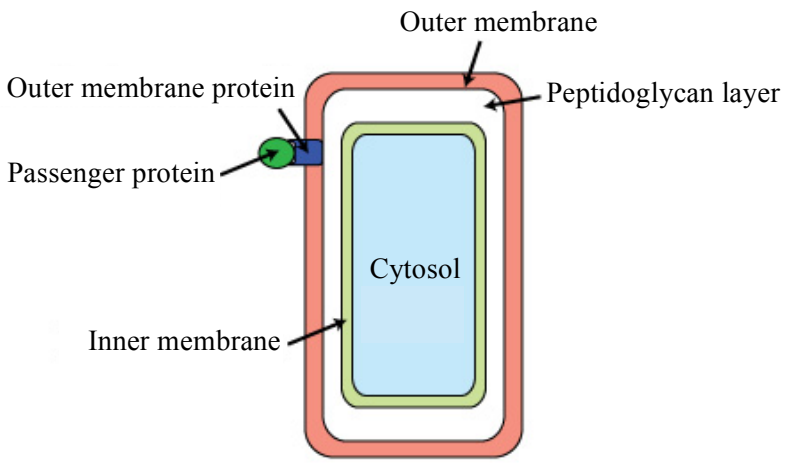

Figure 1.10 Gram-negative bacteria cell surface display.

Secondly, gram-positive bacteria such as *Staphylococcus xylosus* or *Staphylococcus carnosus* have been used. They have a thicker cell wall and lack the outer membrane (Figure. 1.11). They are more suitable to apply for cell catalysts and adsorbents because of cell wall rigidity. *Bacillus* and *Staphylococcus* strains have been commonly used.

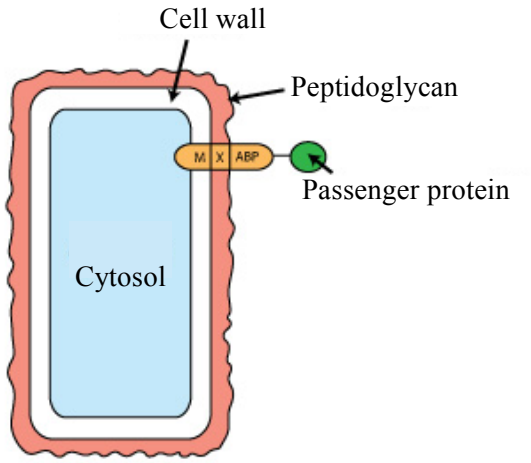

Figure 1.11 Gram-positive bacteria cell surface display.

Library sizes of 10^9-10^{11} can be obtained and screened. On the other hand, a major concern is a protein folding issue (*vide infra*). In addition, *E. coli* does not have the machinery capable of post-translational modifications, such as glycosylation, necessary for functional expression of eukaryotic proteins.

1.4.3 Yeast Surface Display

Yeast display has also been used to improve affinity, specificity, expression, stability, and catalytic activity for various foreign proteins [54]. The Aga1-Aga2 protein complex in *Saccharomyces cerevisiae* has been used as anchors for protein display (Figure. 1.12). These proteins are covalently connected to the cell wall [41, 55]. This display system has been utilized for presentation of various proteins such as green fluorescent protein (GFP), blue fluorescent protein (BFP), the hepatitis B virus antigen, and glucoamylase [56, 57].

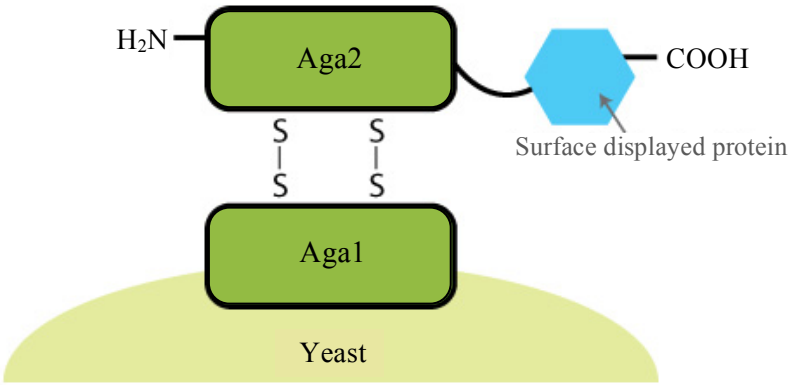

Figure 1.12 Yeast surface display. The surface displayed protein of interest is fused by its N-terminus to the C-terminus of Aga2 protein.

There are several advantages in yeast surface display for protein engineering. Yeast can display large proteins up to 500 amino acids; whereas, a filamentous phage is limited to small peptides. Yeast can perform post-translational modifications. Hence, they are suitable for functional expression of eukaryotic proteins that need glycosylation for

protein folding [54]. On the other hand, a potential drawback of yeast surface display is the smaller library size of 10^6-10^7, which is due to low transformation efficiency. Furthermore, protein folding can be a problem (*vide infra*).

1.4.4 Ribosome Display

Ribosome display is cell free evolution technology to create proteins libraries (Figure. 1.13). The DNA library contains all the signals for transcription and translation. In ribosome display, the translated protein remains connected to the ribosome because there is no stop codon. As a result, a ternary complex of mRNA, ribosome, and protein produce is used for selection [58].

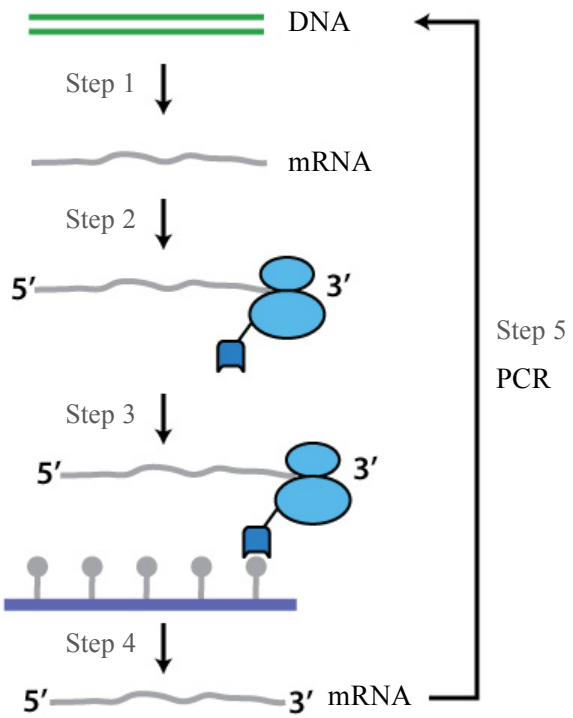

Figure 1.13 Ribosome display for screening for protein libraries. Step 1. DNA library contains the T7 promoter, ribosome binding site, and stem-loops. Step 2. The mRNA is translated. Translation is stopped by cooling to 4°C, and the protein is screened for function. Step 3. Libraries are screened. Step 4. The mRNA is isolated. Step 5. The mRNA is transcribed to cDNA with reverse transcriptase.

Ribosome display has been used to screen antibody libraries [59], peptides [60], proteins with increased stability [61]. An advantage of ribosome display is that large libraries up to 10^{12}-10^{13} can be screened. However, there are some issues, which include protein misfolding, instability mRNA-ribosome-protein complex, and disulfide bonds formation [62].

1.4.5 mRNA Display

Another *in vitro* evolution technology is mRNA display for protein and peptide selections (Figure. 1.14).

Like ribosome display, mRNA display produces libraries up to 10^{12}-10^{13}. As a result, rare sequences can be identified. The mRNA display system has advantage over the ribosome display. The covalent mRNA-protein complex linked by puromycin has resistance to harsh environments. A shortcoming of mRNA display is purification of the protein-puromycin-DNA-mRNA from the ribosome [62].

The mRNA display technique has been used to create libraries of heavy domains and single-chain antibodies as well as select linear and constrained peptides [62]. Furthermore, selections in mRNA display system can identify polypeptide substrates [63] and cellular polypeptides [64] for signaling proteins and small molecular drugs.

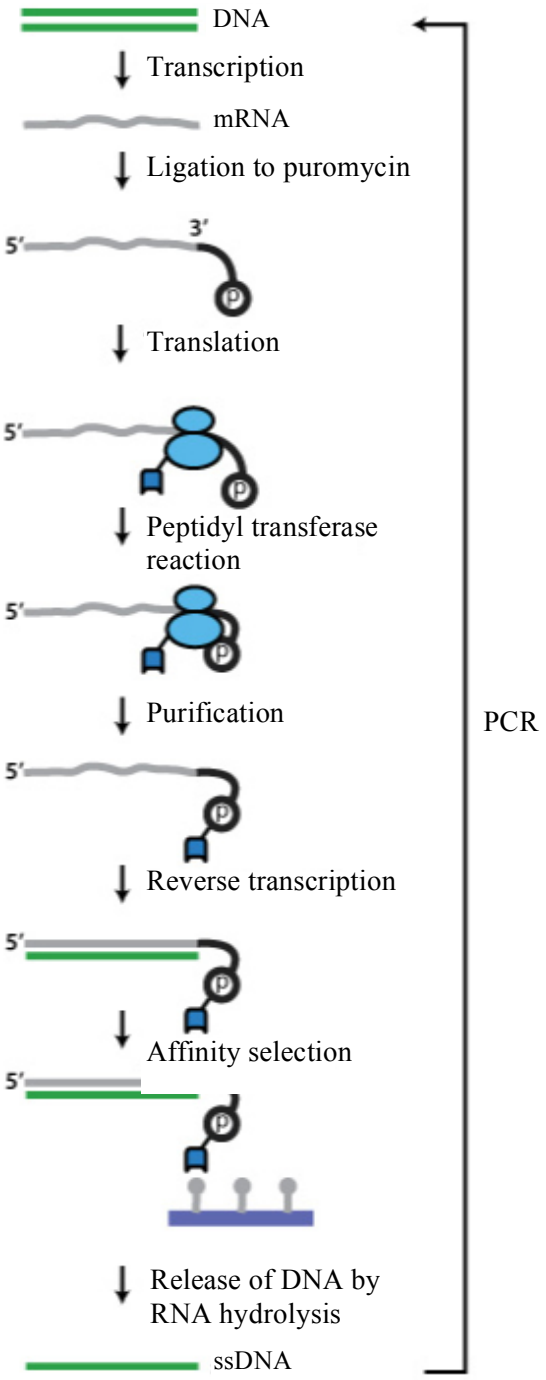

Figure 1.14 mRNA display. Step 1. The DNA library is transcribed to mRNA. Step 2. Puromycin is linked to the mRNA. Step 3. Translation is done *in vitro*. Step 4. Translation is stopped at the linker region. Puromycin binds to the ribosome. Step 5. Protein is transferred to puromycin. Step 6. mRNA is transcribed. Step 7. Selection for desired properties. Step 8. Isolate DNA. Step 9. Synthesize double stranded DNA by PCR.

1.4.6 Spore Display

Protein display methods have revolutionized protein engineering in academic and industrial settings. However, these technologies suffer several limitations, which have been discussed above. More importantly, there are two significant issues; protein folding and cell viability. Initially, protein must be folded properly for function. In *E. coli* display, the protein is expressed in cytoplasm, which has a reducing environment. This hinders correct disulfide bond formation. In addition, the unfolded peptide must cross the inner membrane, peptidoglycan layer, and the outer membrane. Again, protein folding is a concern. Next, screening proteins for extreme properties, such as organic solvent resistance or thermal stability, will destroy the cell. This will also occur when assaying with toxic substrates. As a result, the microorganism cannot be cultured, and the genotype/phenotype connection will be lost.

Spore display may solve protein folding and cell viability issues. Protein folding concerns may be bypassed due to the natural sporulation process [(65)] (Figure. 1.15). First, the vegetative cell divides into two compartments, the mother cell and forespore. The mother cell nurtures the formation of the spore. Spore coat proteins are synthesized in the mother cell and they are deposited to form the coat. In short, proteins found on the surface of the spore do not have to cross membranes. In addition, the mother cell contains ATP-dependent chaperone protein to assist in protein folding [(36)].

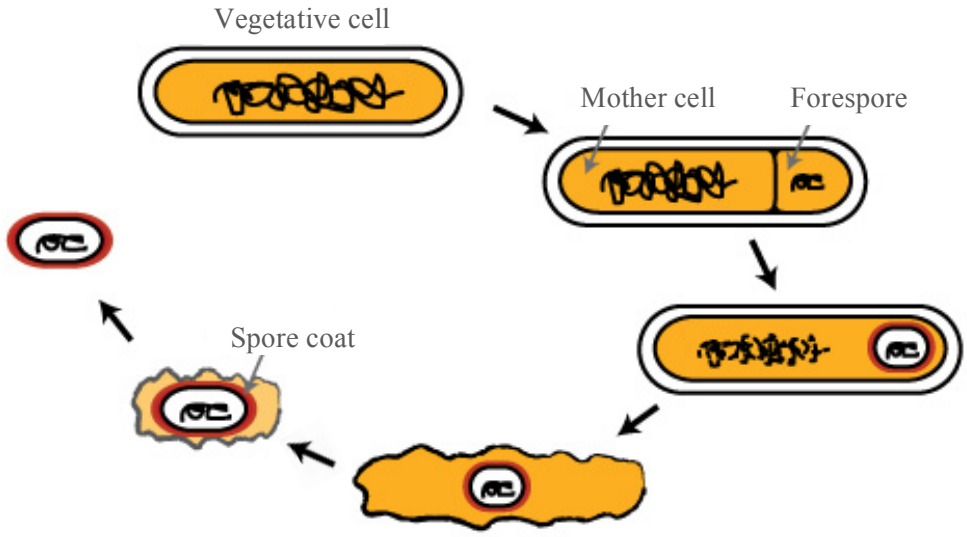

Figure 1.15 Sporulation in *Bacillus Subtilis*.

Second, they are capable of enduring harsh physical and chemical conditions such as heat, radiation, ultraviolet, desiccation, and oxidizers. Spores remain viable under these conditions, while microorganism such as yeast and *E. coli* cannot. As a result, screening protein with extreme properties can be achieved, and the genotype/phenotype connection remains intact.

Spore display may also have additional advantages. In general, immobilized proteins [(66)] have some economical and technological benefits. They are separated easily from the reaction mixture, and the protein stability is increased. For protein immobilization, it is typically expressed, purified, and attached to an inert material. However, proteins are "pre-immobilized" during the sporulation process.

Surface display on *B. subtilis* has been used in biotechnological and pharmaceutical applications [(36)] such as vaccines, biosensors, whole cell catalysts, and bioabsorbants for toxic substances [(66)]. Most recently, spores have been shown to a

suitable platform for directed evolution [67]. *B. subtilis* is convenient organism for protein display. The genome is known and they can be easily manipulated with molecular biology techniques. Furthermore, spores can be easily produced in large quantities. Lastly, they are safe to use and have been developed as additives for foods and drugs.

Spore Display of G-Protein Coupled Receptors: Human Parathyroid Hormone Receptor 1 (huPTH1R)

As mentioned above, obtaining high-resolution crystal structures is a major obstacle towards understanding the molecular mechanisms of GPCR constitutive activity and activation. One significant challenge is acquiring a sufficient amount of protein to crystallize because most GPCRs are expressed at low levels in native tissue. Hence, a suitable recombinant expression system must be developed to produce correctly folded protein, and insect and COS-1 mammalian cells have been used for this purpose [68]. *E. coli* has been also used to generate GPCRs [68]. However, the proteins are expressed as inclusion bodies and they require detergents and other chemical additives for solubilization and refolding.

Spore display offers the opportunity to employ directed evolution methods to stabilize GPCRs. This evolutionary approach would complement other stability methods, such as antibodies binding [6, 14], T4 lysozyme grafting [14, 15], and other protein engineering efforts were also used. One notable example was the evolution of GPCRs for higher expression and stability, which was achieved in two steps [69]. First, a library of GPCRs was expressed in the inner membrane of *E. coli*, and GPCRs with increased expression level were sorted with Fluorescence-Activated Cell Sorting, FACS. Second, the improved variants were screened for thermal stability using microtiter plates. The

clones were expressed and tagged with biotin, and then they were partially purified using streptavidin coated magnetic beads. Finally, they were assayed for enhanced thermal stability.

Spore display of GPCRs may be a general tool for engineering these proteins by overcoming several concerns. First, spore display results in "purified" protein on the spore surface because each spore will contain a unique member of the library. Next, the displayed GPCRs are expected to be unfolded and they need to be solubilized and refolded. As mentioned above, this step requires detergents and other chemical additives. Spores can endure extreme environments and they still remain viable. Hence, spores are not affected during the refolding process. On the other hand, the refolding conditions are not compatible for the more established protein display formats, such as *E. coli* and yeast, because the cell wall may rupture. This would result losing in the genotype/phenotype connection. Finally, only the GPCRs that can be expressed and assayed will be displayed. For example, GPCRs with rare codon usage in *B. subtilis* may be removed during the library creation and screening procedure. In short, spore display can be a general tool to engineer proteins.

The goal of this project is to design and create a system for spore display. The molecular biology will be performed in order to fuse a GPCR, human parathyroid hormone receptor 1 (huPTH1R), to the spore coat protein, CotC. HuPTH1R is vital in regulating calcium and phosphate levels in the blood [(70)]. Defects in huPTH1R can result in dwarfism, bone tumors, and failure of tooth eruption.

CHAPTER 2

DESIGNING A SYSTEM FOR DISPLAYING HUMAN PARATHYROID HORMONE RECEPTOR 1 ON THE SPORE COAT OF *BACILLUS SUBTILIS*

In this chapter, the design is described for the construction of a system to display G-protein coupled receptors on spore coat of *Bacillus subtilis*. More specifically, the cloning design and molecular biology will be outlined.

2.1 Materials

Analytical regent grade chemicals were purchased from Sigma-Aldrich (St. Louis, MO), BD (Franklin Lakes, NJ), Research Products International Corp. (Mount Prospect, IL), and Invitrogen (Carlsbad, CA). Restriction enzymes were purchased from Invitrogen (Carlsbad, CA) and New England Biolabs (Ipswich, MA). T4 DNA ligase and *Taq* DNA polymerase were from Invitrogen (Carlsbad, CA), and *PfuUltra* HF DNA polymerase was from Ailgent technologies (Santa Clara, CA). Primers were procured from Eurofins MWG Operon (Huntsville, AL). QuikChange Site-Directed Mutagenesis Kit was purchased from Ailgent technologies (Santa Clara, CA). QIAprep spin miniprep kit, QIAquick PCR Purification Kit, and QIAquick gel extraction kit were purchased from Qiagen (Valencia, CA). DNA sequencing was performed at Molecular Resource Facility in University of Medicine and Dentistry of New Jersey (Newark, NJ).

2.2 Methods

2.2.1 Remove *Xho*I Restriction Site at Position 7049 Base Pair for Ease of Cloning

The PCR reaction mixture consist of 5µl of 10X reaction buffer, 5 to 50ng template, pDG1730 GFP-CotC, 125ng of pDG1730 *Xho*I forward (pDG1730 *Xho*I-F: 5'-GGAAGTATCCAGCTCCAGGTCGGGCCGCG-3') and pDG1730 *Xho*I reverse primer (pDG1730 *Xho*I-R: 5'-CGCGGCCCGACCTGGAGCTGGATACTTCC-3'), respectively, 1µl of dNTP mix and ddH_2O to a final volume of 50µl. Then, 1µl *pfuTurbo* DNA polymerase (2.5U/µl) was added. The PCR consisted of 1 cycle at 95°C for 30 seconds and 12 cycles at 95°C for 30 seconds, 55°C for 1 minute and 68°C for 4 minutes. After the PCR reaction, the product were directly digested with 1µl of the *Dpn*I restriction enzyme (10U/µl), and incubated at 37°C for an hour. After digestion, it was transformed into XL1-Blue supercompetent cells by heat shock. The transformed cells were plated on the Luria–Bertani (LB) plate containing ampicillin (50µg/mL) and incubated at 37°C overnight. The mutated plasmid was isolated using QIAprep spin miniprep kit, and both original and mutated plasmids were digested with *Xho*I and *EcoR*I to check and compare the results. The mutation was verified by agarose gel electrophoresis.

2.2.2 Amplification of Human Parathyroid Hormone Receptor 1

Human parathyroid hormone receptor 1 (huPTH1R) was amplified from the plasmid pET15b huPTH1R (Aline Desmyster, Architecture et Fonction des Macromolécules Biologiques, UMR 6098, CNRS, and Universités of Marseille, F-13288 Marseille Cedex 09, France) [(68)]. The reaction mixture contain 5µl of 10X *PfuUltra* HF reaction buffer, 1µl

of dNTP mix, 100ng/µl of pET15b – huPTH1R template, 100ng/µl each of huPTH1R – *Hind*III-F (5'-GGCAAGCTTACATAAGGAGGAACTACTATGGGCAGCAGCCATC ATC-3') and huPTH1R – *Xho*I-R (5'-CGGCTCGAGCATGACTGTCTCCCACTCTTCC -3'), 1µl of *PfuUltra* HF DNA polymerase (2.5U/µl), and up to 50µl with sterile ddH_2O. The PCR consisted of 1 cycle at 95°C for 2 minutes, 30 cycles at 95°C for 30 seconds, 65°C for 30 seconds and 72°C for 4 minutes, and then 1 cycle 72°C for 10 minutes. The PCR amplification products were purified using QIAquick PCR Purification Kit and analyzed on a 1% (w/v) agarose gel.

2.2.3 Construction of pDG1730 HuPTH1R-CotC

2.2.3.1 Digestion of pDG1730 GFP-CotC and HuPTH1R PCR Fragments. The reaction mixture contained *Hind*III, 10X buffer, each of pDG1730 GFP-CotC or huPTH1R PCR fragments from above, and to a final volume 50µl. Both mixtures were incubated at 37°C for 3 hours. The digested pDG1730 GFP-CotC and huPTH1R fragments were purified using QIAquick PCR Purification, and then second digestion with *Xho*I was performed. The reaction mixture included *Xho*I, 10X buffer, digested pDG1730 GFP-CotC and huPTH1R PCR fragments, respectively, and up to 50µl with sterile ddH_2O. Incubation conditions were at 37°C for 3 hours again. Finally, the products were purified using QIAquick gel extraction kit to select desired size of fragments.

2.2.3.2 Ligation of HuPTH1R and pDG1730 CotC. Purified huPTH1R (insert) and pDG1730 (vector) were ligated (Figure. 2.1 A). The 20µl ligation reaction contained 4µl of 5X ligase reaction buffer, insert and vector (1:1, 3:1, 6:1, and 9:1), and 0.1 unit of

T4 DNA ligase. The ligation was performed at 25°C for 1 hour. The final plasmid construct, pDG1730 huPTH1R-CotC (Figure. 2.1 B), was created.

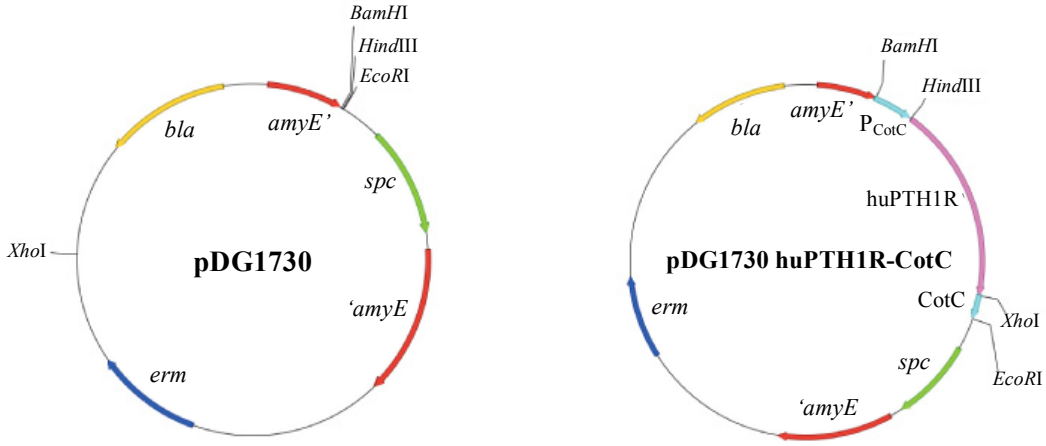

Figure 2.1 Plasmid maps. **(A)** pDG1730. **(B)** pDG1730 huPTH1R-CotC. Genes; *amyE'*: encodes front of α-amylase; '*amyE*: encodes back of α-amylase; *spc*: encodes spectinomycin adenyltransferase (spectinomycin resistance); *bla*: encodes β-lactamase (ampicillin resistance); *erm*: encodes rRNA adenine N-6-methyltransferase (erythromycin resistance). *BamH*I, *Hind*III, *EcoR*I and *Xho*I are the restriction sites.

2.2.3.3 Transformation of pDG1730 huPTH1R-CotC. The ligated plasmid was transformed into XL10-gold ultracompetent cells by electroporation. The transformed cells were spread on the LB agar plate containing ampicillin (50μg/mL), and incubated at 37°C overnight. The plasmid was isolated using QIAprep spin miniprep kit. The insert was verified with DNA sequencing (UMDNJ).

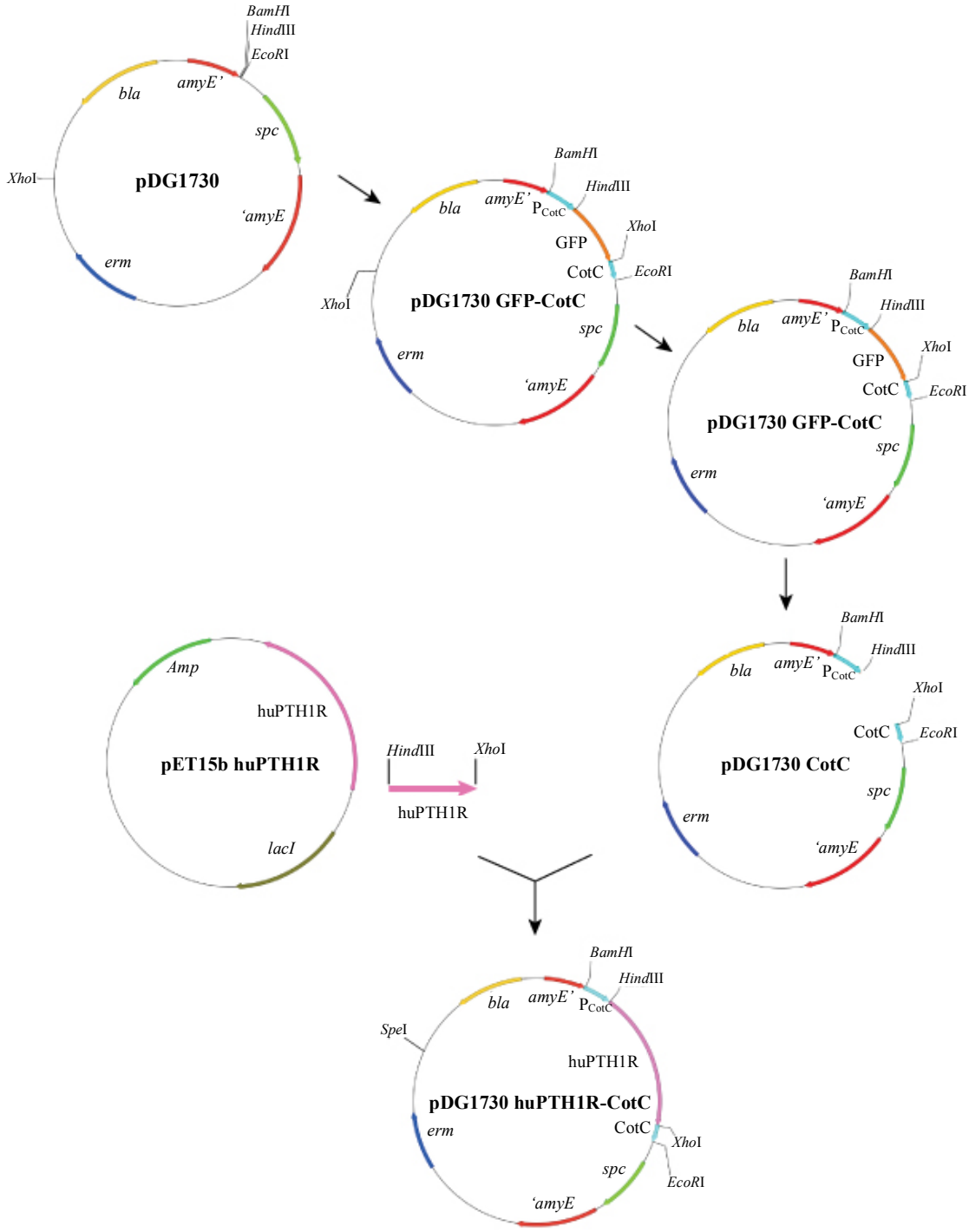

Figure 2.2 Cloning strategies.

2.2.4 *Bacillus subtilis* Transformation

The plasmid pDG1730 huPTH1R-CotC was linearized by digestion with *Spe*I at 37°C for 3 hours and used to transform competent cells of the CotC knockout *B. subtilis* strain (Figure. 2.3). The *B. subtilis* cells were plated on the LB agar plate containing spectinomycin (100μg/mL) and chloramphenicol (5μg/mL), and then they were incubated at 37°C overnight. The plasmid pDG1730 huPTH1R-CotC was integrated into the non-essential *amyE* gene by double crossover recombination. This integration was verified using PCR and the primers used were huPTH1R – *Hind*III-F and huPTH1R – *Xho*I-R. The reaction and cycling condition was the same as for the amplification of huPTH1R. Next, wild-type *B. subtilis* and *B. subtilis* transformed with pDG1730 huPTH1R-CotC were spread on the LB agar plate containing spectinomycin (100μg/mL) and analyzed by growth on the plate with appropriate antibiotics. Finally, genomic DNA was isolated, and the gene was sequenced (UMDNJ).

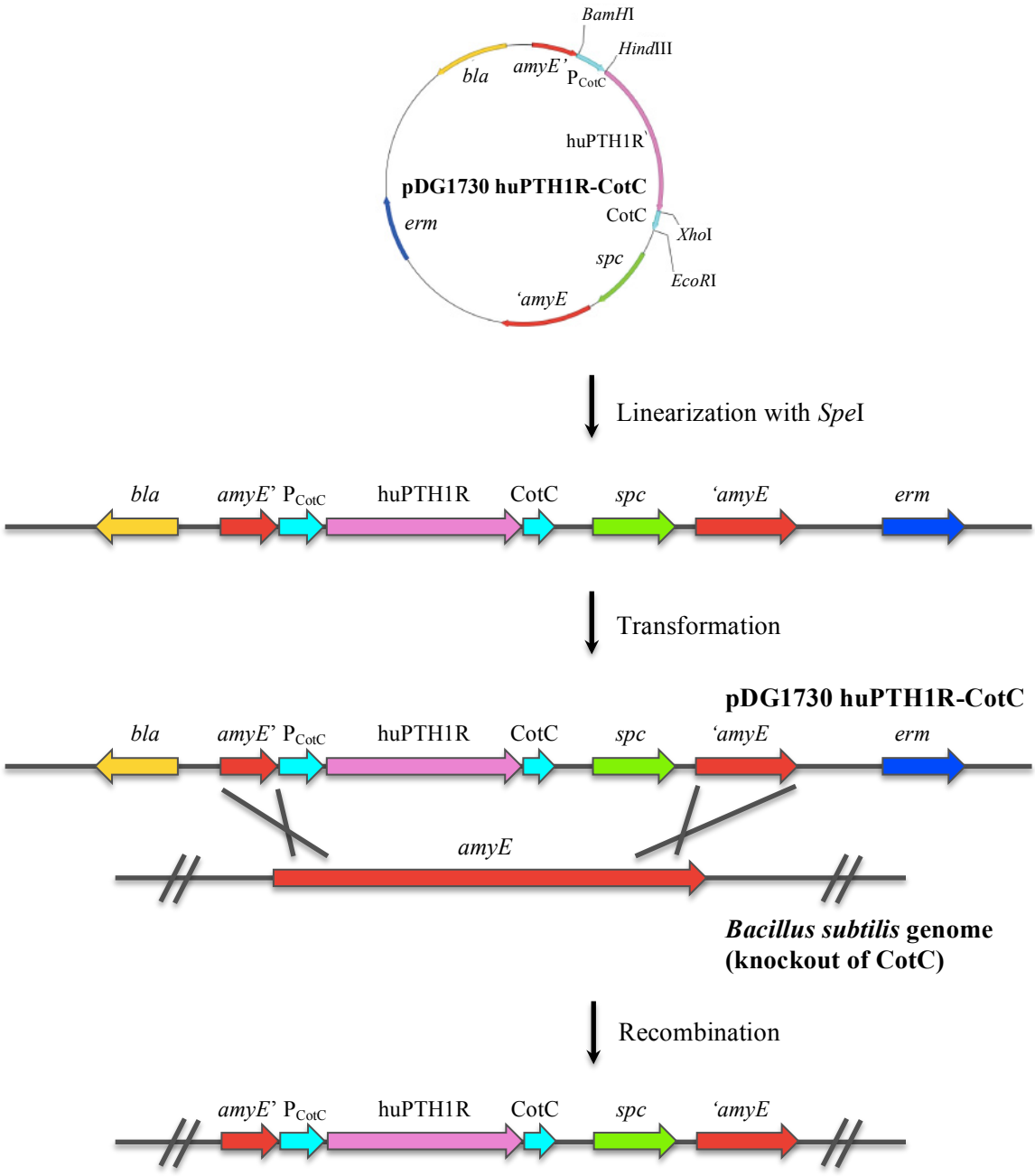

Figure 2.3 Integration of pDG1730 huPTH1R-CotC into *Bacillus subtilis* genome.

CHAPTER 3

RESULTS AND DISCUSSION

3.1 Remove *Xho*I Restriction Site at Position 7049 Base Pair for Ease of Cloning

The plasmid pDG1730 GFP-CotC (Patrick Eichenberger, Department of Biology, New York University) contains two *Xho*I restriction sites (CTCGAG). A guanine to cytosine point mutation was performed at position 7049 using QuikChange Site-Directed Mutagenesis. It was necessary to have only one *Xho*I restriction site for ease of cloning. To verify the result of removing *Xho*I restriction site, the plasmid pDG1730 GFP-CotC and the mutated plasmid was digested with *Xho*I and *EcoR*I (Figure. 3.1).

The pDG1730 GFP-CotC and the mutated plasmids were digested with *EcoR*I. It is expected to generate one linear fragment, 8903bp (Figure. 3.1, Lanes 2 and 3) because there is only one restriction site. On the other hand, the plasmid pDG1730 GFP-CotC was digested with *Xho*I. It is expected to result in two fragments, 5308 bp and 3595 bp (Figure. 3.1, Lanes 4). The mutated plasmid has only one *Xho*I restriction site, and the digestion is expected to have a single 8903 bp fragment (Figure. 3.1, Lanes 5).

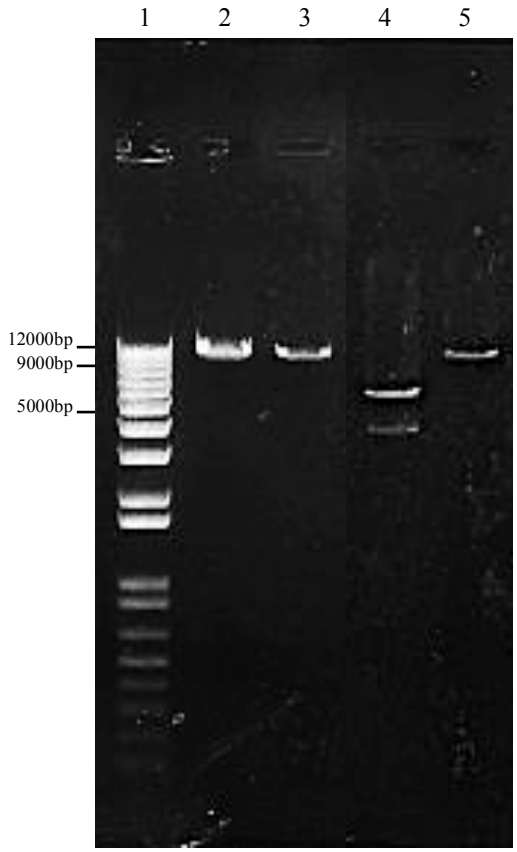

Figure 3.1 Analysis of mutation of *Xho*I restriction site by gel electrophoresis. Lane 1: 1kb DNA plus ladder, Lane 2: *EcoR*I digestion of pDG1730 GFP-CotC original plasmid, Lane 3: *EcoR*I digestion of QuikChange site-directed mutation of pDG1730 GFP-CotC plasmid, Land 4: *Xho*I digestion of pDG1730 GFP-CotC original plasmid, Lane 5: *Xho*I digestion of QuikChange site-directed mutation of pDG1730 GFP-CotC plasmid.

3.2 Amplification of Human Parathyroid Hormone Receptor 1

The huPTH1R gene was successfully amplified from the plasmid pET15b huPTH1R (Aline Desmyster, Architecture et Fonction des Macromolécules Biologiques, UMR 6098, CNRS, and Universités of Marseille, F-13288 Marseille Cedex 09, France) [(68)] with huPTH1R – *Hind*III-F and huPTH1R – *Xho*I-R, which were the forward and reverse primers, respectively. The forward primer incorporated a *Hind*III restriction site at the 5' end, while the reverse primer integrated an *Xho*I restriction site at the 3' end. The PCR

reaction was purified using QIAquick gel extraction kit, and PCR products were analyzed on the 1% (w/v) agarose gel. The expected size of huPTH1R was 1806bp (Figure. 3.2, Lane 3).

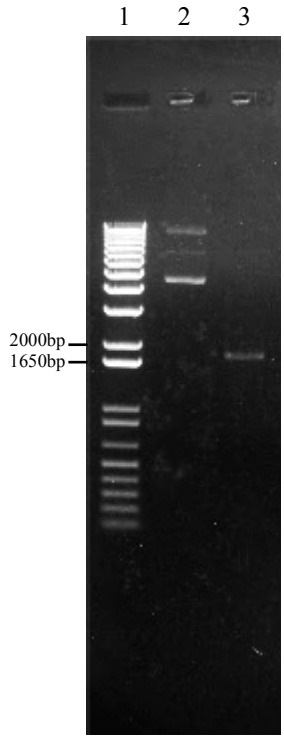

Figure 3.2 Analysis of huPTH1R gene by gel electrophoresis. Lane 1: 1kb DNA plus ladder, Lane 2: pET15b huPTH1R original plasmid, Lane 3: huPTH1R PCR products.

3.3 Construction of pDG1730 HuPTH1R-CotC

The plasmid pDG1730 huPTH1R-CotC was constructed. First, the pDG1730 GFP-CotC and huPTH1R PCR product were digested with *Hind*III and *Xho*I. This created sticky ends in order to ligate the vector (digested pDG1730 GFP-CotC) and the insert (digested huPTH1R PCR product). The digestions were analyzed by agarose gel electrophoresis. The digested insert shows one band at 1806 bp (Figure. 3.3, Lane 3).

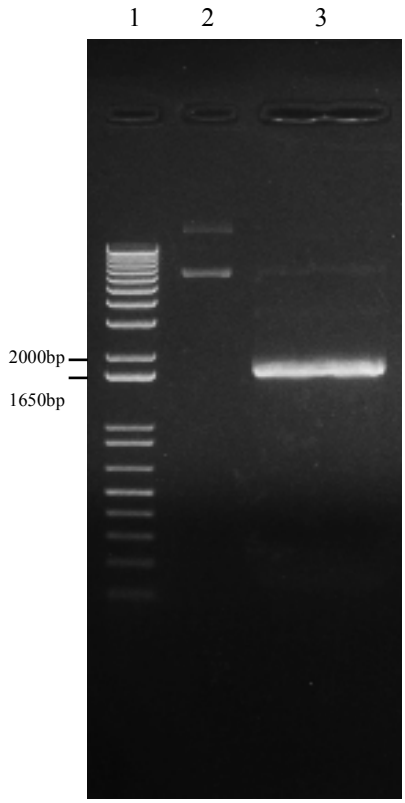

Figure 3.3 Analysis of huPTH1R PCR fragments after *Xho*I digestion by gel electrophoresis. Lane 1: 1kb DNA plus ladder, Lane 2: pET15b huPTH1R original plasmid, Lane 3: huPTH1R PCR fragments.

The double digestion of pDG1730 GFP-CotC resulted in two bands. The band at 738bp corresponds to the coding region for GFP, and the band at 8165 bp was remaining part of the plasmid pDG1730 CotC, which was used as the vector (Figure. 3.4, Lanes 2 and 3).

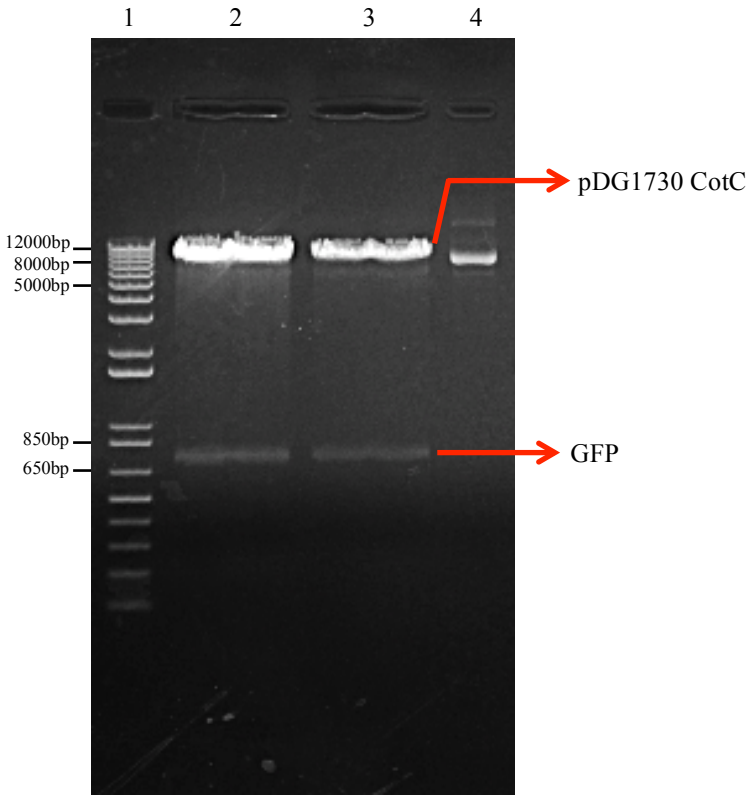

Figure 3.4 Analysis of pDG1730 GFP-CotC after *Xho*I digestion by gel electrophoresis. Lane 1: 1kb DNA plus ladder, Lanes 2 and 3: pDG1730 CotC and GFP, Lane 4: pDG1730 GFP-CotC original plasmid.

The vector and insert were cut out and purified from the gel using a QIAquick gel extraction kit. Separate ligation reactions were done with insert to vector ratio of 1:1, 3:1, 6:1, and 9:1. Then, the ligated plasmids were transformed into XL10-gold ultracompetent cells by electroporation and plated on the LB agar plate containing ampicillin (50µg/mL). Several colonies were selected, and plasmids were isolated using QIAprep spin miniprep kit. Successful ligation was determined by PCR amplification of the insert, huPTH1R. A clone was found in the 3:1 insert to vector reaction, which displayed an 1806 bp fragment (Figure. 3.5, Lane 6). This plasmid was requested DNA sequencing (UMDNJ), and the results verified presence of the insert (Appendix A).

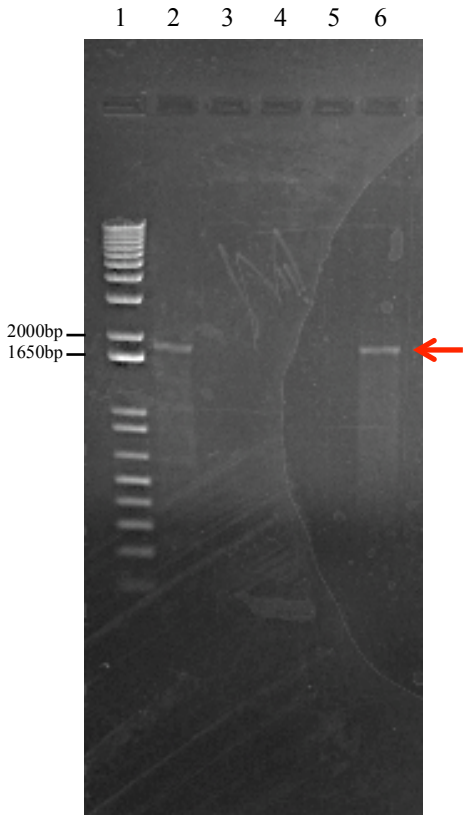

Figure 3.5 Analysis of huPTH1R after transformation by gel electrophoresis. Lane 1: 1kb DNA plus ladder, Lane 2: huPTH1R PCR products for positive control, Lane 3 ~ 6: huPTH1R PCR products after transformation.

3.4 *Bacillus subtilis* Transformation

The plasmid pDG1730 huPTH1R-CotC was linearized with the restriction enzyme *Spe*I, and it was transformed into competent cells of the CotC knockout *B. subtilis* strain. The *B. subtilis* cells were spread on the LB agar plate containing spectinomycin (100μg/mL) and chloramphenicol (5μg/mL). Several colonies were chosen, and the genomic DNA was isolated. PCR was performed with the genomic DNA, and a product corresponding with the correct size of huPTH1R PCR (1794 bp) was detected by agarose gel

electrophoresis (Figure. 3.6, Lane 3). In addition, genomic DNA was isolated and sequenced (UMDNJ) for the presence of the huPTH1R gene (Appendix B).

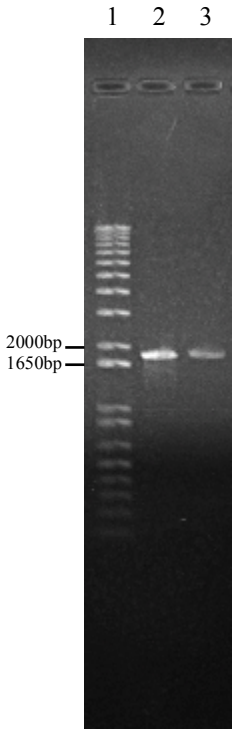

Figure 3.6 Analysis of recombination of pDG1730 huPTH1R CotC by gel electrophoresis. Lane 1: 1kb DNA plus ladder, Lane 2: huPTH1R PCR products for positive control, Lane 3: huPTH1R PCR products after *B. subtilis* transformation.

Next, integration of pDG1730 huPTH1R-CotC resulted in conferring antibiotic resistance to spectinomycin resistance. Wild type of *B. subtilis* did not grow on the LB agar plate containing spectinomycin (100μg/mL), while the transformed *B. subtilis* strain did (Figure. 3.7).

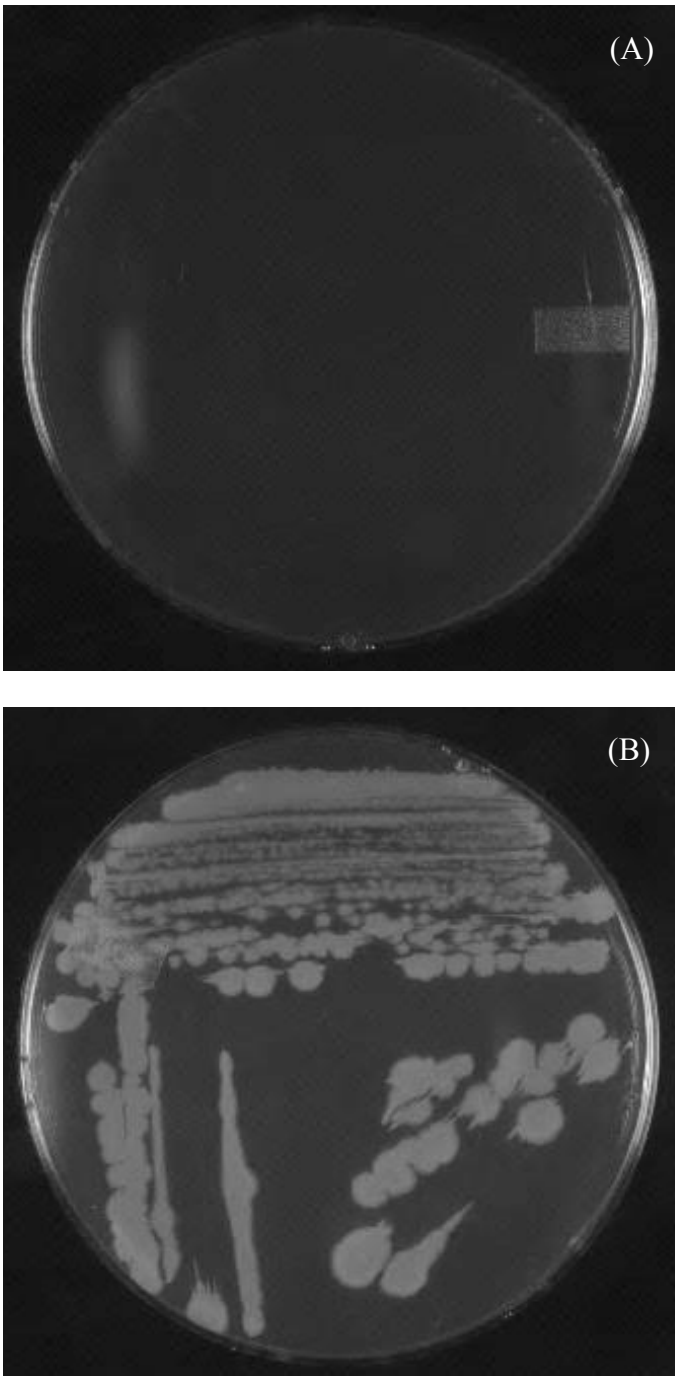

Figure 3.7 Growth characteristics of *B. subtilis* with LB agar plates containing spectinomycin (100µg/mL). (**A)** Wild-type *B. subtilis*. (**B)** *B. subtilis* strain transformed with pDG1730 huPTH1R-CotC.

CHAPTER 4

CONCLUSION

In conclusion, integration of huPTH1R into *B. subtilis* was successfully done. First, molecular biology was used to create the plasmid pDG1730 huPTH1R-CotC that fused a GPCR (huPTH1R) to a spore coat protein (CotC). Next, pDG1730 huPTH1R-CotC was transformed into *B. subtilis* display to integrate the GPCR into the genome. This work represents the first system for GPCR display on the spore coat. Spore display overcomes many of hurdles found in "typical" protein display systems. Furthermore, this system can be used a general method for engineering and optimizing membrane proteins by directed evolution. The next goals are to demonstrate proper GPCR display on the spore coat, and then the protein will be evolved for stability.

APPENDIX A

SEQUENCING ANALYSIS RESULTS

Figure A.1 to A.8 show DNA sequencing results of pDG1730 huPTH1R-CotC.

(A)

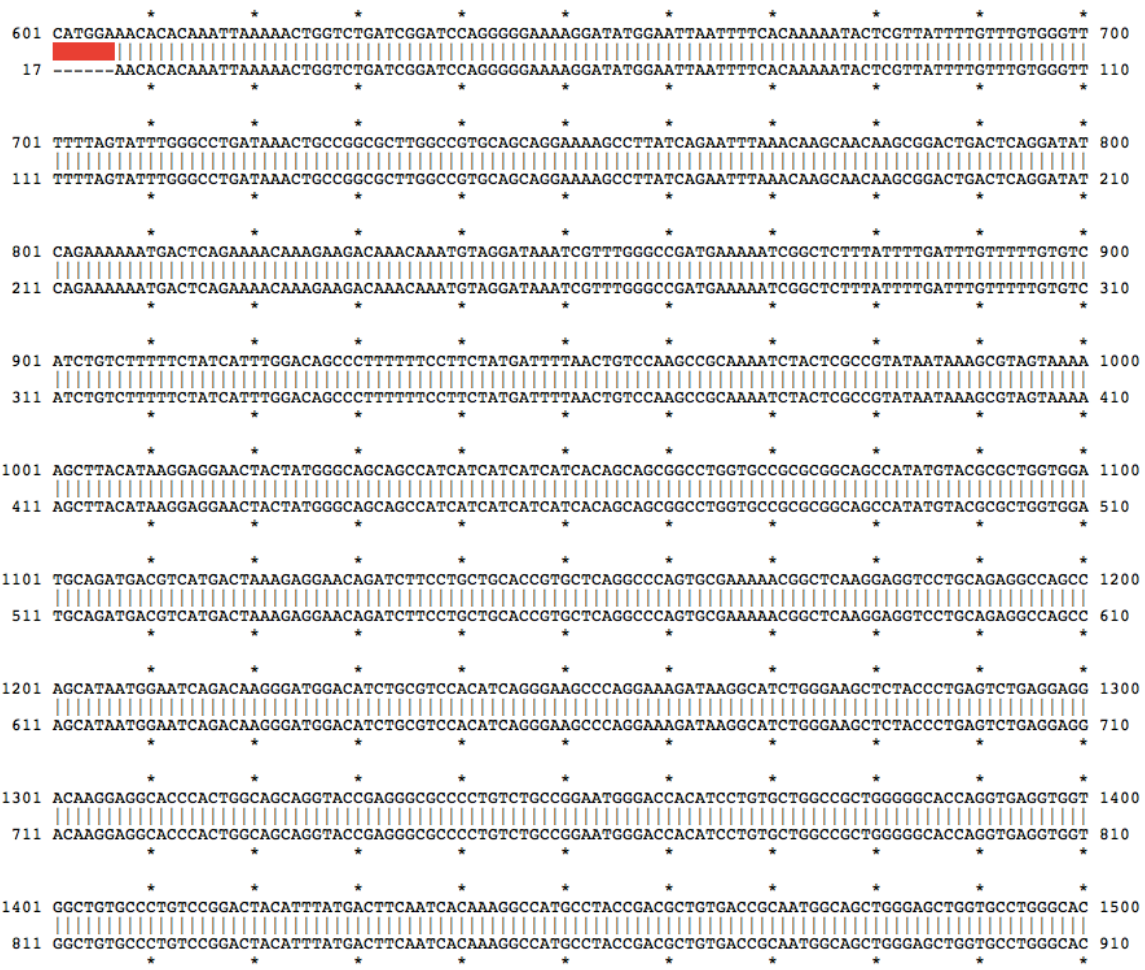

Figure A.1 DNA sequencing results of pDG1730 huPTH1R-CotC. **(A)** Top strand is the DNA coding region from the promoter of CotC to CotC, P_{CotC}-huPTH1R-CotC DNA. The bottom strand represents the DNA sequencing results using the primer seq-huPTH1R CotC-F1 (5'-TATGCCGCGATTTCCAATGAGG-3'). Nucleotide 641 is the start of P_{CotC} and 3015 is end of CotC. This alignment represents 641 ~ 1500.

(B)

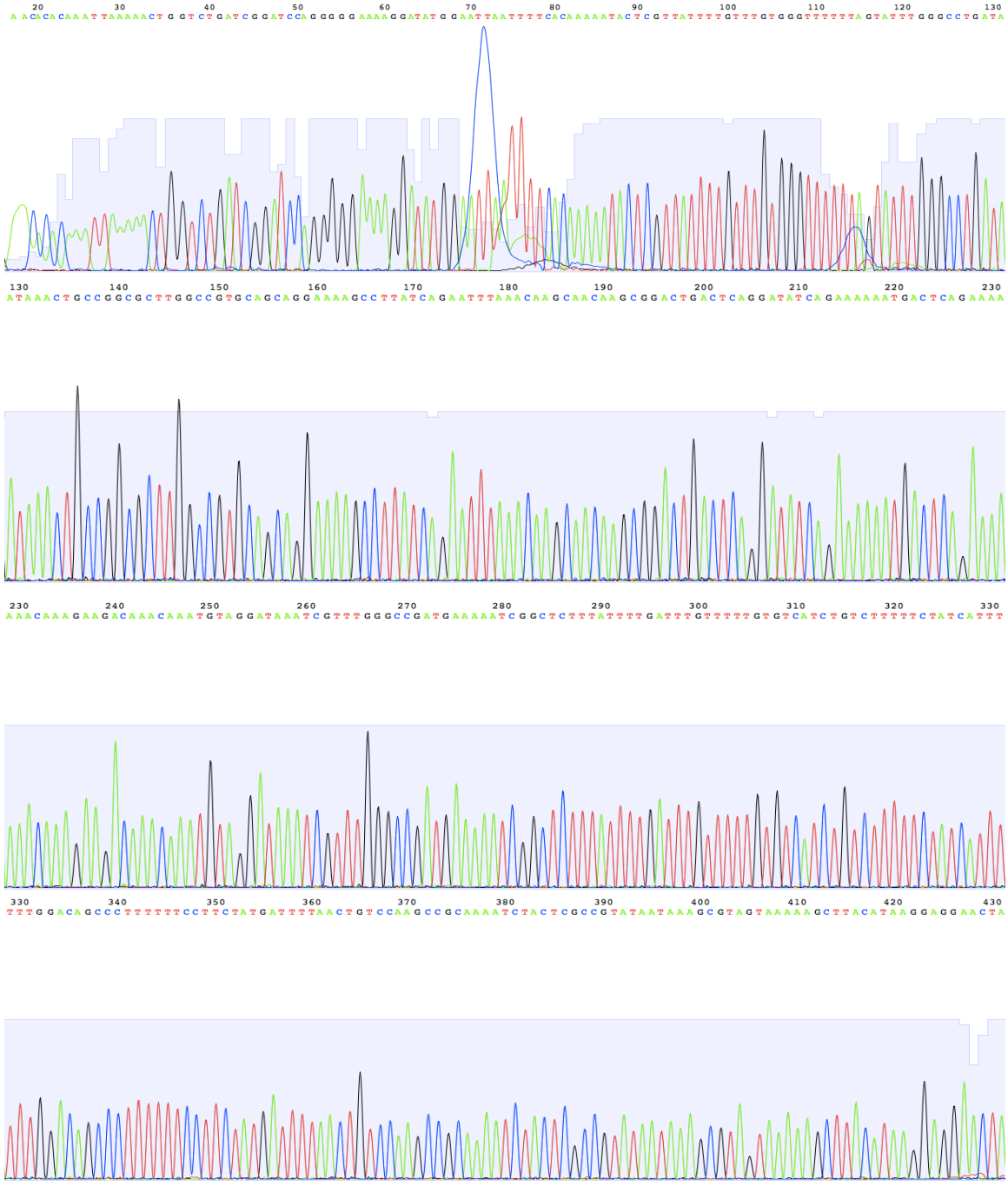

Figure A.1 DNA sequencing results of pDG1730 huPTH1R-CotC. **(B)** DNA sequencing traces were done with the primer seq-huPTH1R CotC-F1. (Continued)

(A)

Figure A.2 DNA sequencing results of pDG1730 huPTH1R-CotC. **(A)** Top strand is the DNA coding region from the promoter of CotC to CotC, P_{CotC}-huPTH1R-CotC DNA. The bottom strand represents the DNA sequencing results using the primer seq-huPTH1R CotC-F2 (5'-GGCAAGCTTACATAAGGAGGAACTACTATGGGCAGCAGCCATCA TC-3'). Nucleotide 641 is the start of P_{CotC} and 3015 is end of CotC. This alignment represents 1046 ~ 1900.

(B)

Figure A.2 DNA sequencing results of pDG1730 huPTH1R-CotC. **(B)** DNA sequencing traces were done with the primer seq-huPTH1R CotC-F2. (Continued)

(A)

Figure A.3 DNA sequencing results of pDG1730 huPTH1R-CotC. **(A)** Top strand is the DNA coding region from the promoter of CotC to CotC, P_{CotC}-huPTH1R-CotC DNA. The bottom strand represents the DNA sequencing results using the primer seq-huPTH1R CotC-F3 (5'-CACAACAGGACGTGGGCCAACTACAG-3'). Nucleotide 641 is the start of P_{CotC} and 3015 is end of CotC. This alignment represents 1560 ~ 2400.

(B)

Figure A.3 DNA sequencing results of pDG1730 huPTH1R-CotC. **(B)** DNA sequencing traces were done with the primer seq-huPTH1R CotC-F3. (Continued)

(A)

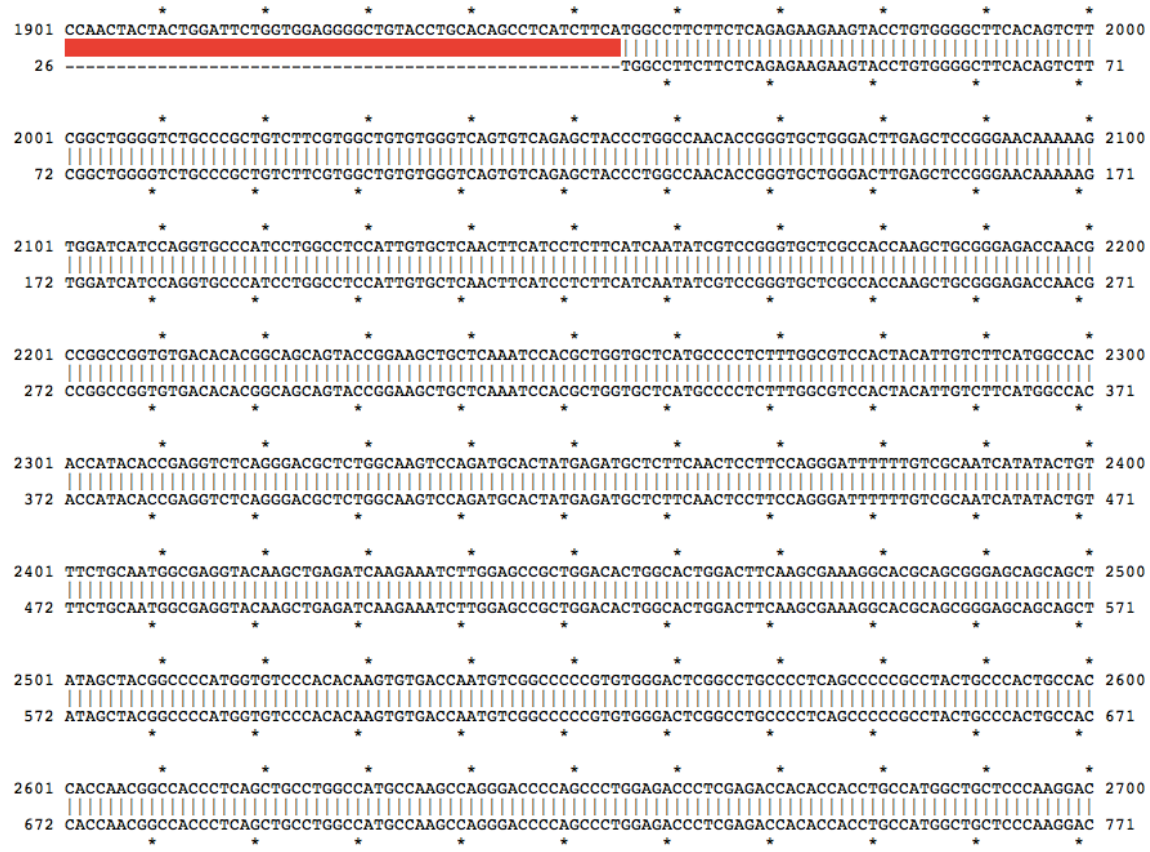

Figure A.4 DNA sequencing results of pDG1730 huPTH1R-CotC. **(A)** Top strand is the DNA coding region from the promoter of CotC to CotC, P_{CotC}-huPTH1R-CotC DNA. The bottom strand represents the DNA sequencing results using the primer seq-huPTH1R CotC-F4 (5'-GGCCACCAACTACTACTGGATTCTGG-3'). Nucleotide 641 is the start of P_{CotC} and 3015 is end of CotC. This alignment represents 1955 ~ 2700.

(B)

Figure A.4 DNA sequencing results of pDG1730 huPTH1R-CotC. **(B)** DNA sequencing traces were done with the primer seq-huPTH1R CotC-F4. (Continued)

(A)

Figure A.5 DNA sequencing results of pDG1730 huPTH1R-CotC. **(A)** Top strand is the DNA coding region from the promoter of CotC to CotC, P_{CotC}-huPTH1R-CotC DNA. The bottom strand represents the DNA sequencing results using the primer seq-huPTH1R CotC-F5 (5'-GCAATGGCGAGGTACAAGCTGAGATC-3'). Nucleotide 641 is the start of P_{CotC} and 3015 is end of CotC. This alignment represents 2471 ~ 3015.

(B)

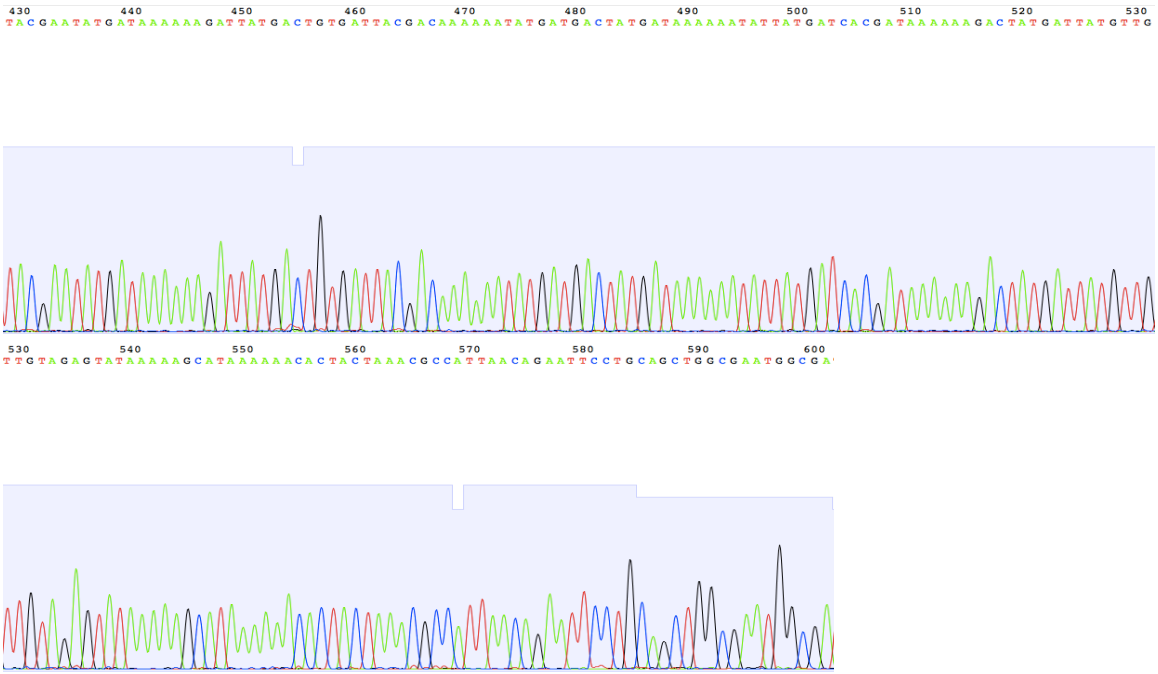

Figure A.5 DNA sequencing results of pDG1730 huPTH1R-CotC. **(B)** DNA sequencing traces were done with the primer seq-huPTH1R CotC-F5. (Continued)

(A)

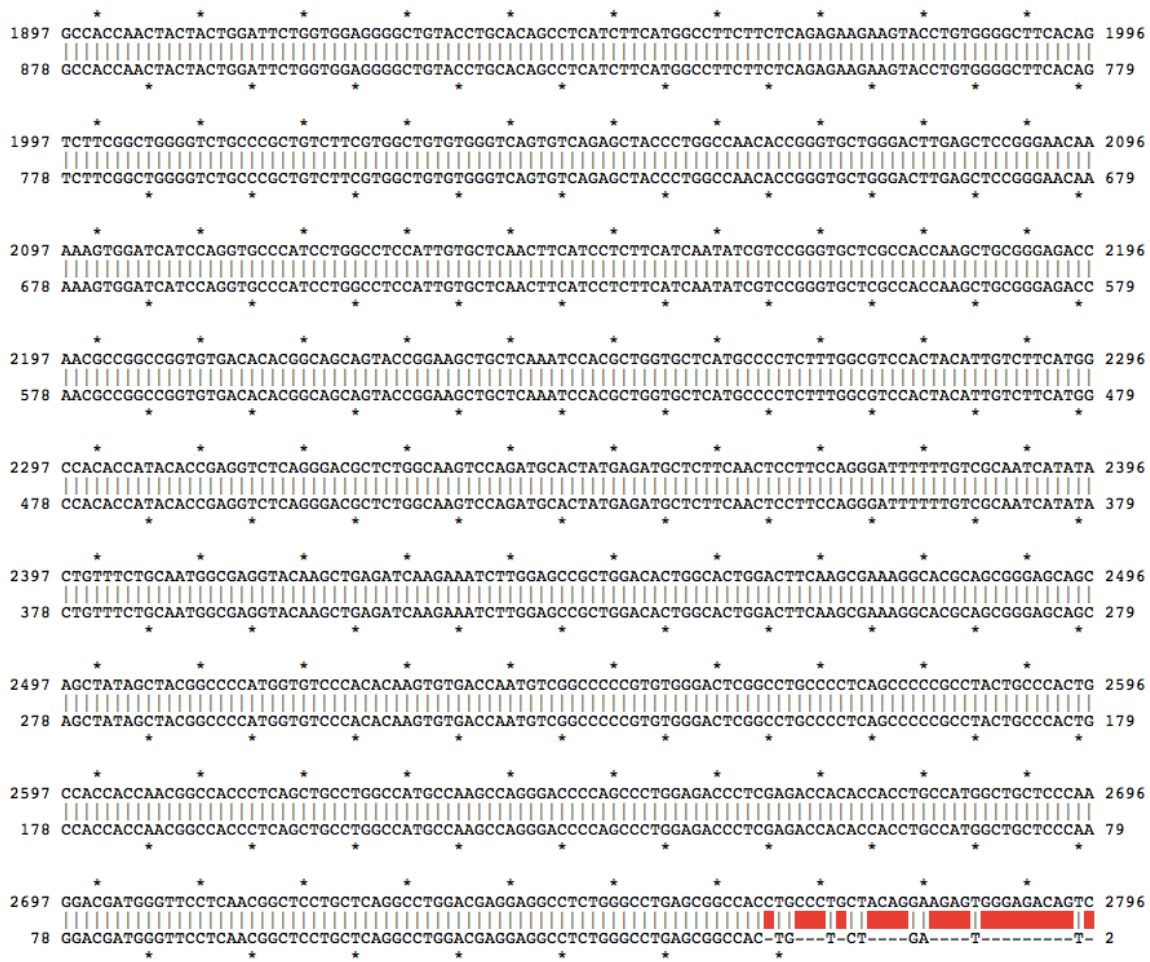

Figure A.6 DNA sequencing results of pDG1730 huPTH1R-CotC. **(A)** Top strand is the DNA coding region from the promoter of CotC to CotC, P_{CotC}-huPTH1R-CotC DNA. The bottom strand represents the DNA sequencing results using the primer seq-huPTH1R CotC-R2 (5'-CGGCTCGAGCATGACTGTCTCCCACTCTTCC-3'). Nucleotide 641 is the start of P_{CotC} and 3015 is end of CotC. This alignment represents 1892 ~ 2764.

(B)

Figure A.6 DNA sequencing results of pDG1730 huPTH1R-CotC. **(B)** DNA sequencing traces were done with the primer seq-huPTH1R CotC-R2. (Continued)

(A)

Figure A.7 DNA sequencing results of pDG1730 huPTH1R-CotC. **(A)** Top strand is the DNA coding region from the promoter of CotC to CotC, P_{CotC}-huPTH1R-CotC DNA. The bottom strand represents the DNA sequencing results using the primer seq-huPTH1R CotC-R4 (5'-CCAGAATCCAGTAGTAGTTGGTGGCC-3'). Nucleotide 641 is the start of P_{CotC} and 3015 is end of CotC. This alignment represents 1034 ~ 1879.

(B)

Figure A.7 DNA sequencing results of pDG1730 huPTH1R-CotC. **(B)** DNA sequencing traces were done with the primer seq-huPTH1R CotC-R4. (Continued)

(A)

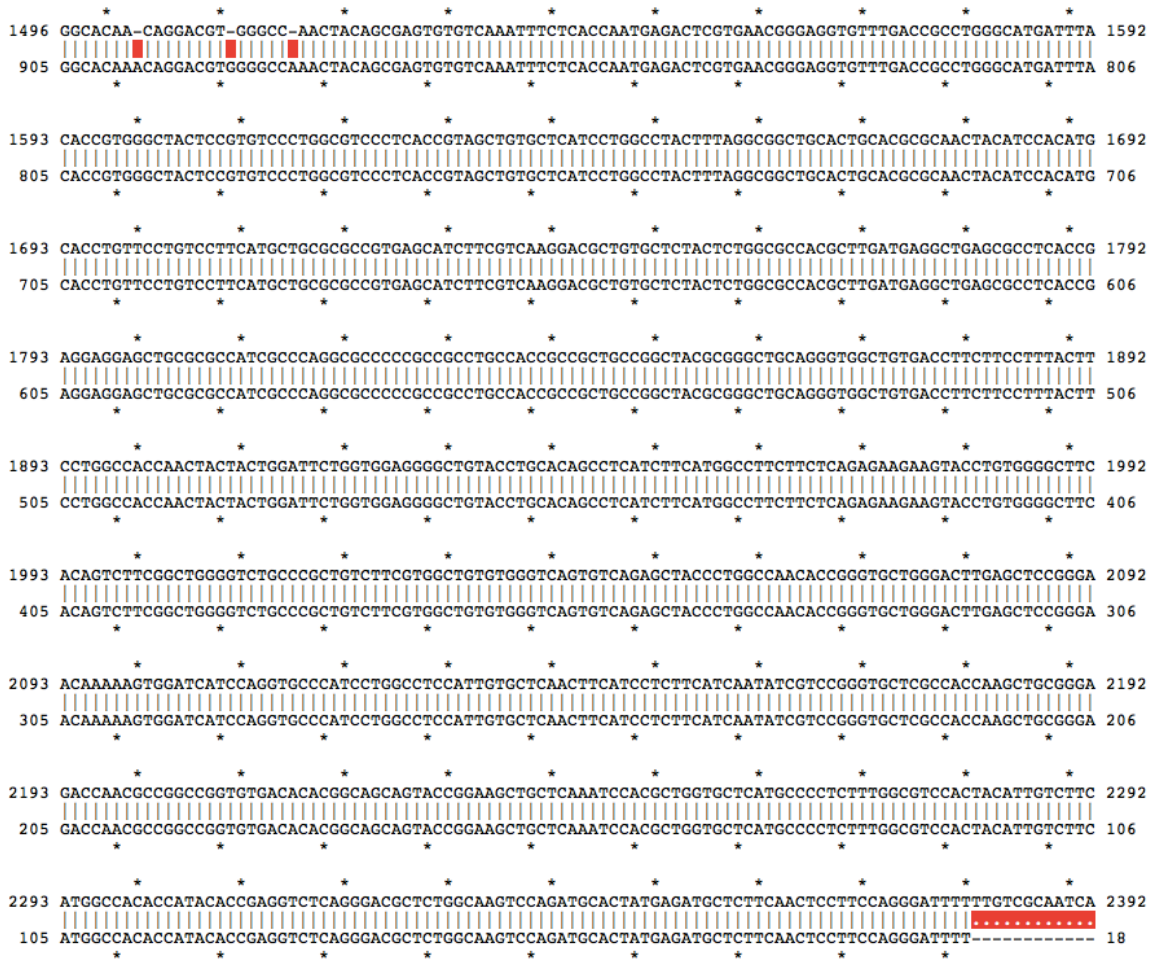

Figure A.8 DNA sequencing results of pDG1730 huPTH1R-CotC. **(A)** Top strand is the DNA coding region from the promoter of CotC to CotC, P_{CotC}-huPTH1R-CotC DNA. The bottom strand represents the DNA sequencing results using the primer seq-huPTH1R CotC-R5 (5'-GATCTCAGCTTGTACCTCGCCATTGC-3'). Nucleotide 641 is the start of P_{CotC} and 3015 is end of CotC. This alignment represents 1516 ~ 2380.

(B)

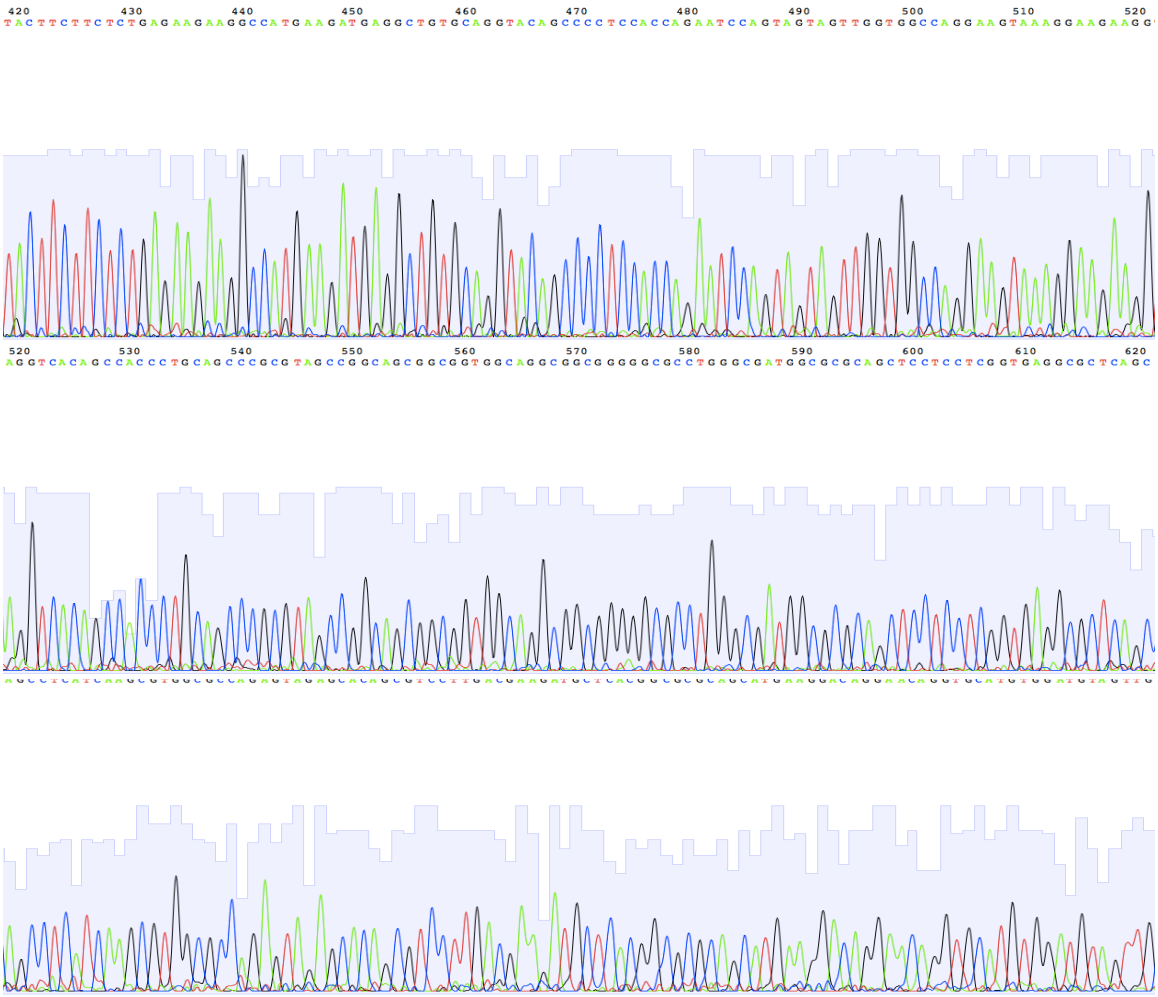

Figure A.8 DNA sequencing results of pDG1730 huPTH1R-CotC. **(B)** DNA sequencing traces were done with the primer seq-huPTH1R CotC-R5. (Continued)

APPENDIX B

SEQUENCING ANALYSIS RESULTS

Figure B.1 to B.8 show genomic DNA sequencing results of integration of pDG1730 huPTH1R-CotC.

(A)

```
  1 ~~~~~~~~~~~~~~~~~~~~~~~~~~~~~~~~~~~~~~~~~~~~~~~~~~~AGGGGGAAAAGGATATGGAATTAATTTTCACAAAAATACTCGTTATTTT  49
  1 CATCAACTGGAACATGGAACACACAAATTAAAAACTGGTCTGATCGGATCCAGGGGGAAAAGGATATGGAATTAATTTTCACAAAAATACTCGTTATTTT 100

 50 GTTTGTGGGTTTTTTAGTATTTGGGCCTGATAAACTGCCGGCGCTTGGCCGTGCAGCAGGAAAAGCCTTATCAGAATTTAAACAAGCAACAAGCGGACTG 149
101 GTTTGTGGGTTTTTTAGTATTTGGGCCTGATAAACTGCCGGCGCTTGGCCGTGCAGCAGGAAAAGCCTTATCAGAATTTAAACAAGCAACAAGCGGACTG 200

150 ACTCAGGATATCAGAAAAAATGACTCAGAAAACAAAGAAGACAAACAAATGTAGGATAAATCGTTTGGGCCGATGAAAAATCGGCTCTTTATTTTGATTT 249
201 ACTCAGGATATCAGAAAAAATGACTCAGAAAACAAAGAAGACAAACAAATGTAGGATAAATCGTTTGGGCCGATGAAAAATCGGCTCTTTATTTTGATTT 300

250 GTTTTTGTGTCATCTGTCTTTTTCTATCATTTGGACAGCCCTTTTTTCCTTCTATGATTTTAACTGTCCAAGCCGCAAAATCTACTCGCCGTATAATAAA 349
301 GTTTTTGTGTCATCTGTCTTTTTCTATCATTTGGACAGCCCTTTTTTCCTTCTATGATTTTAACTGTCCAAGCCGCAAAATCTACTCGCCGTATAATAAA 400

350 GCGTAGTAAAAAGCTTACATAAGGAGGAACTACTATGGGCAGCAGCCATCATCATCATCATCACAGCAGCGGCCTGGTGCCGCGCGGCAGCCATATGTAC 449
401 GCGTAGTAAAAAGCTTACATAAGGAGGAACTACTATGGGCAGCAGCCATCATCATCATCATCACAGCAGCGGCCTGGTGCCGCGCGGCAGCCATATGTAC 500

450 GCGCTGGTGGATGCAGATGACGTCATGACTAAAGAGGAACAGATCTTCCTGCTGCACCGTGCTCAGGCCCAGTGCGAAAAACGGCTCAAGGAGGTCCTGC 549
501 GCGCTGGTGGATGCAGATGACGTCATGACTAAAGAGGAACAGATCTTCCTGCTGCACCGTGCTCAGGCCCAGTGCGAAAAACGGCTCAAGGAGGTCCTGC 600

550 AGAGGCCAGCCAGCATAATGGAATCAGACAAGGGATGGACATCTGCGTCCACATCAGGGAAGCCCAGGAAAGATAAGGCATCTGGGAAGCTCTACCCTGA 649
601 AGAGGCCAGCCAGCATAATGGAATCAGACAAGGGATGGACATCTGCGTCCACATCAGGGAAGCCCAGGAAAGATAAGGCATCTGGGAAGCTCTACCCTGA 700

650 GTCTGAGGAGGACAAGGAGGCACCCACTGGCAGCAGGTACCGAGGGCGCCCCTGTCTGCCGGAATGGGACCACATCCTGTGCTGGCCGCTGGGGGCACCA 749
701 GTCTGAGGAGGACAAGGAGGCACCCACTGGCAGCAGGTACCGAGGGCGCCCCTGTCTGCCGGAATGGGACCACATCCTGTGCTGGCCGCTGGGGGCACCA 800

750 GGTGAGGTGGTGGCTGTGCCCTGTCCGGACTACATTTATGACTTCAATCACAAAGGCCATGCCTACCGACGCTGTGACCGCAATGGCAGCTGGGAGCTGG 849
801 GGTGAGGTGGTGGCTGTGCCCTGTCCGGACTACATTTATGACTTCAATCACAAAGGCCATGCCTACCGACGCTGTGACCGCAATGGCAGCTGGGAGCTGG 900
```

Figure B.1 Genomic DNA sequencing results of integration of pDG1730 huPTH1R-CotC. (A) Top strand is the DNA coding region from the promoter of CotC to CotC, P_{CotC}-huPTH1R-CotC DNA. The bottom strand represents the genomic DNA sequencing results using the primer seq-huPTH1R CotC-F1 (5’-TATGCCGCGATTTCC AATGAGG -3’). Nucleotide 1 is the start of P_{CotC} and 2735 is end of CotC. This alignment represents 1 ~ 849.

(B)

Figure B.1 Genomic DNA sequencing results of integration of pDG1730 huPTH1R-CotC. **(B)** Genomic DNA sequencing traces were done with the primer seq-huPTH1R CotC-F1. (Continued)

(A)

Figure B.2 Genomic DNA sequencing results of integration of pDG1730 huPTH1R-CotC. (A) Top strand is the DNA coding region from the promoter of CotC to CotC, P_{CotC}-huPTH1R-CotC DNA. The bottom strand represents the genomic DNA sequencing results using the primer seq-huPTH1R CotC-F2 (5'-GGCAAGCTTACAT AAGGAGGAACTACTATGGGCAGCAGCCATCATC-3'). Nucleotide 1 is the start of P_{CotC} and 2735 is end of CotC. This alignment represents 406 ~ 1375.

(B)

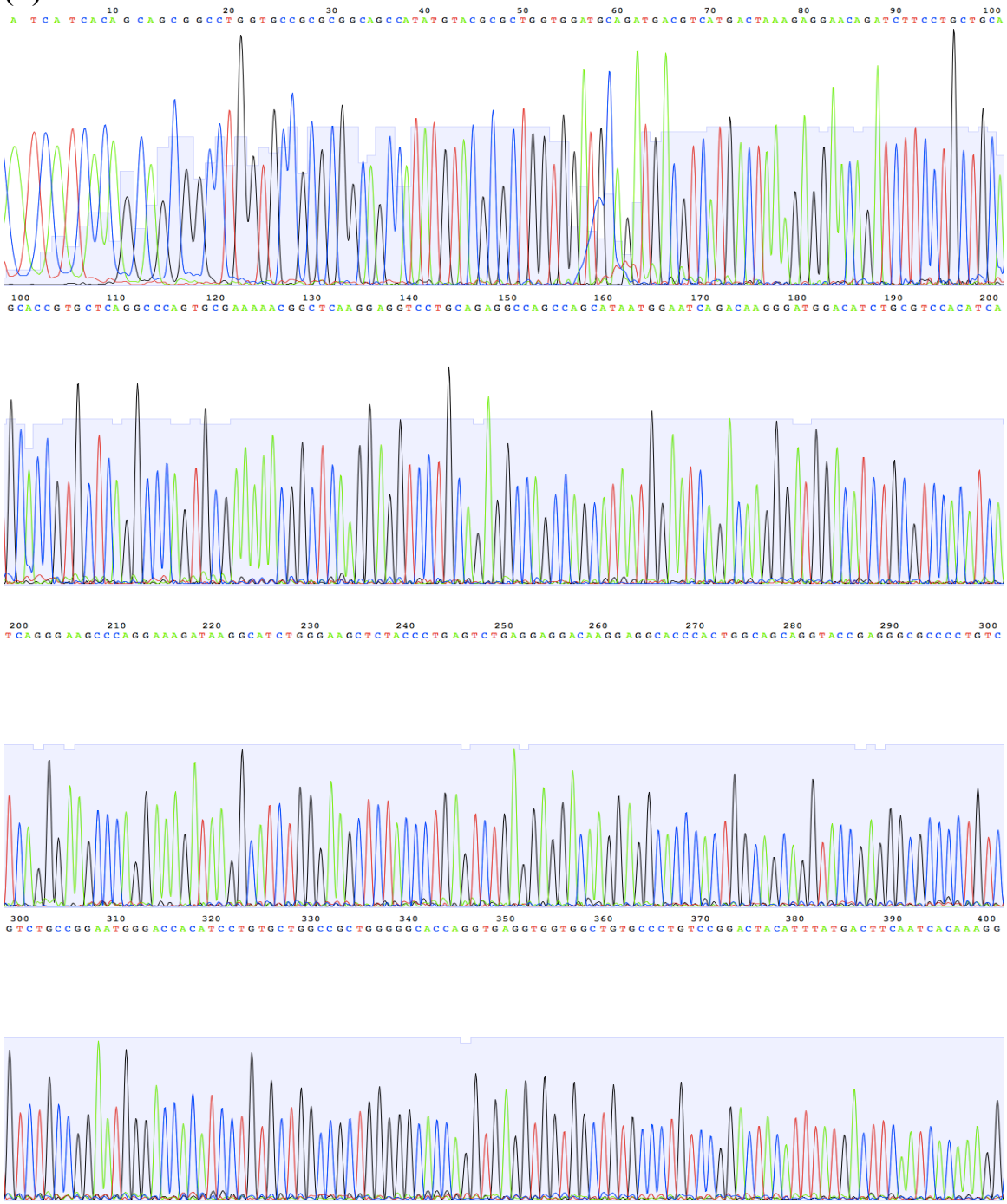

Figure B.2 Genomic DNA sequencing results of integration of pDG1730 huPTH1R-CotC. **(B)** Genomic DNA sequencing traces were done with the primer seq-huPTH1R CotC-F2. (Continued)

(A)

Figure B.3 Genomic DNA sequencing results of integration of pDG1730 huPTH1R-CotC. (A) Top strand is the DNA coding region from the promoter of CotC to CotC, P_{CotC}-huPTH1R-CotC DNA. The bottom strand represents the genomic DNA sequencing results using the primer seq-huPTH1R CotC-F3 (5'-CACAACAGGACGTG GGCCAACTACAG-3'). Nucleotide 1 is the start of P_{CotC} and 2375 is end of CotC. This alignment represents 920 ~ 1802.

(B)

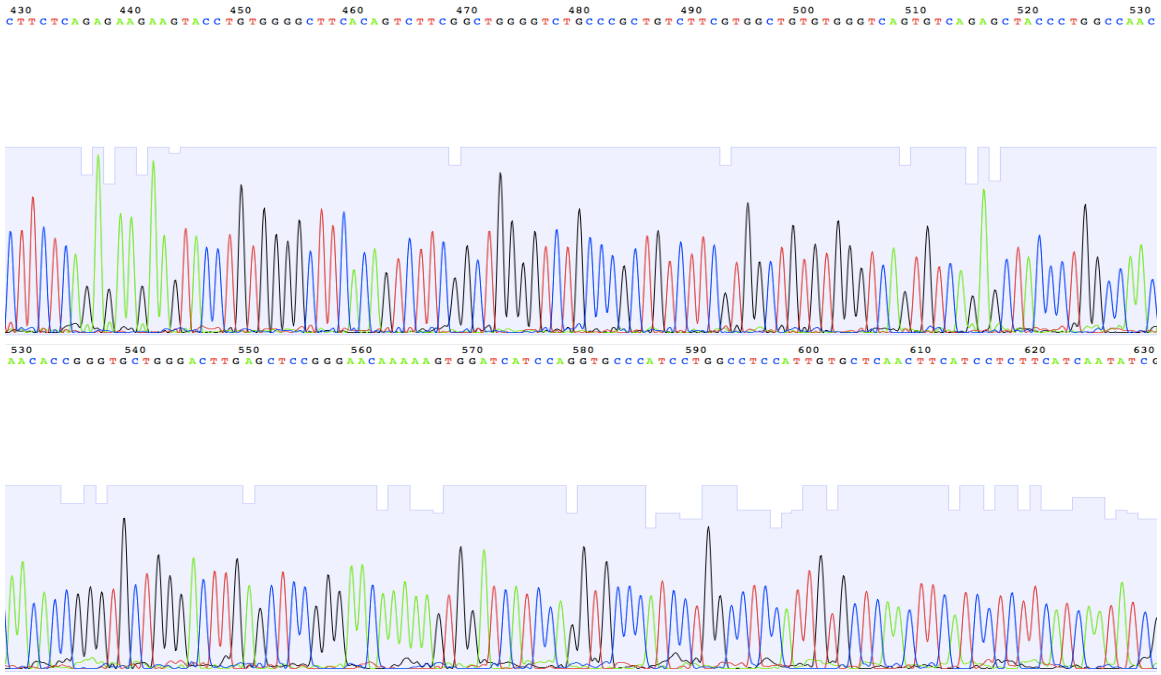

Figure B.3 Genomic DNA sequencing results of integration of pDG1730 huPTH1R-CotC. **(B)** Genomic DNA sequencing traces were done with the primer seq-huPTH1R CotC-F3. (Continued)

(A)

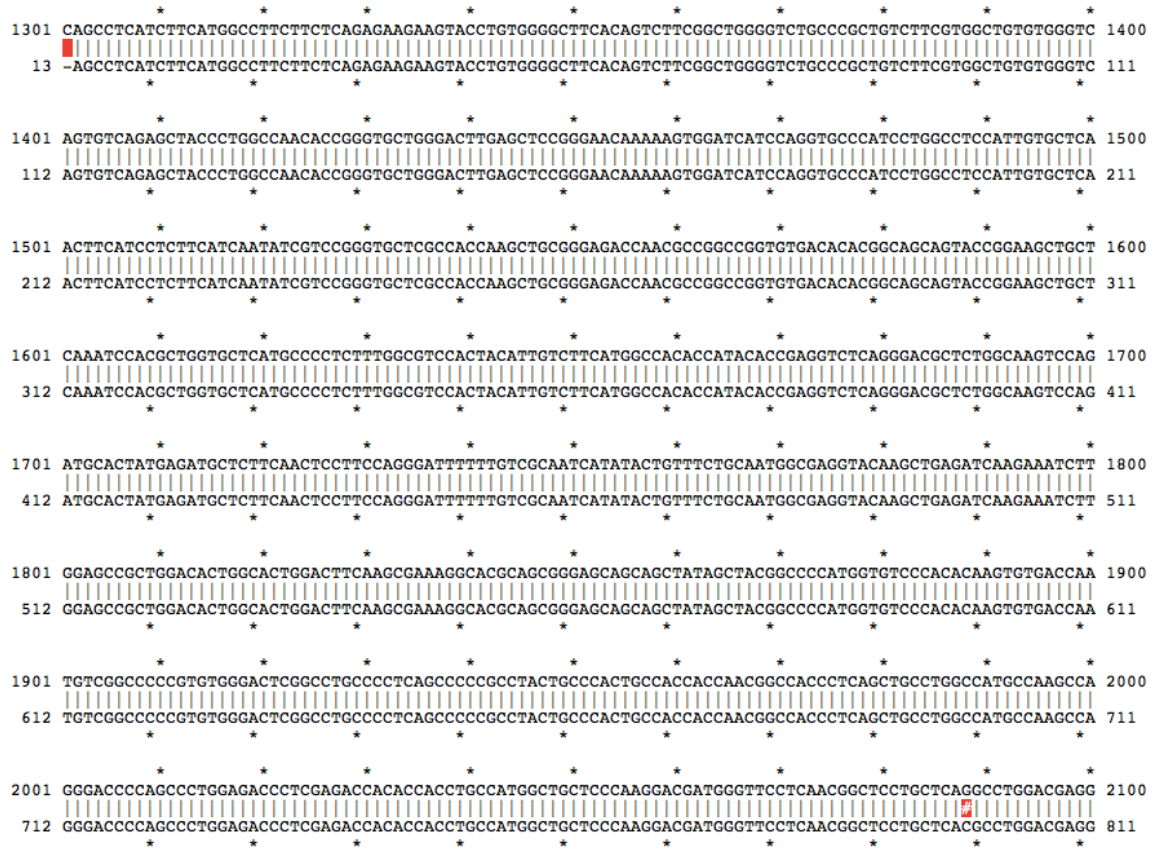

Figure B.4 Genomic DNA sequencing results of integration of pDG1730 huPTH1R-CotC. (A) Top strand is the DNA coding region from the promoter of CotC to CotC, P_{CotC}-huPTH1R-CotC DNA. The bottom strand represents the genomic DNA sequencing results using the primer seq-huPTH1R CotC-F4 (5'-GGCCACCAACTACTA CTGGATTCTGG-3'). Nucleotide 1 is the start of P_{CotC} and 2375 is end of CotC. This alignment represents 1302 ~ 2087.

(B)

Figure B.4 Genomic DNA sequencing results of integration of pDG1730 huPTH1R-CotC. **(B)** Genomic DNA sequencing traces were done with the primer seq-huPTH1R CotC-F4. (Continued)

(A)

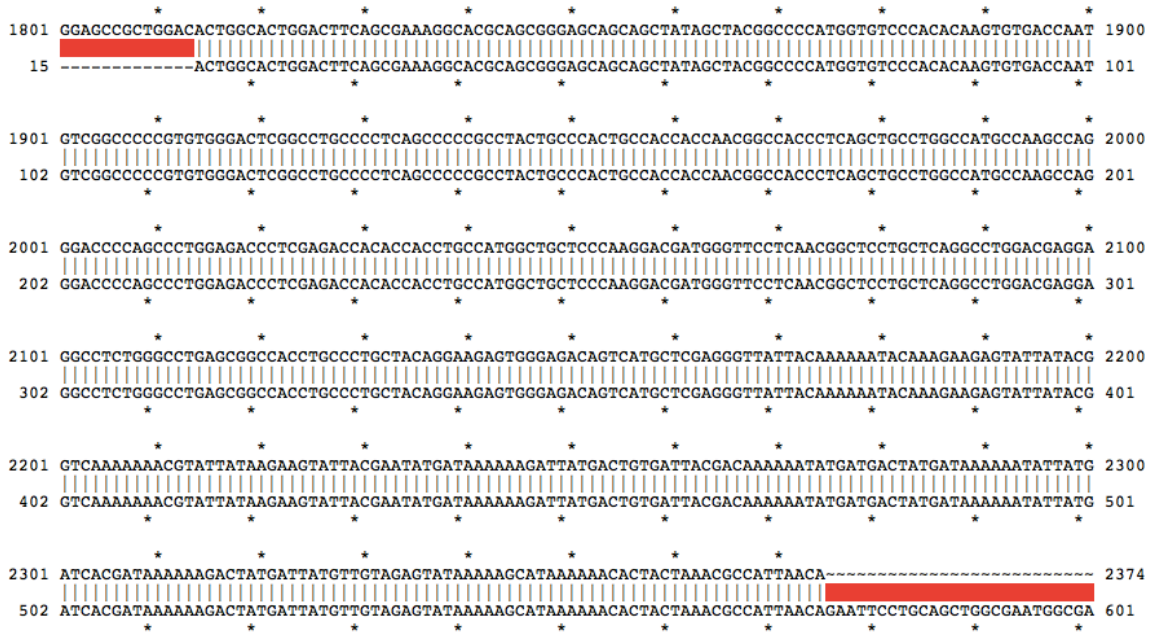

Figure B.5 Genomic DNA sequencing results of integration of pDG1730 huPTH1R-CotC. (A) Top strand is the DNA coding region from the promoter of CotC to CotC, P_{CotC}-huPTH1R-CotC DNA. The bottom strand represents the genomic DNA sequencing results using the primer seq-huPTH1R CotC-F5 (5'-GCAATGGCGAGGTA CAAGCTGAGATC-3'). Nucleotide 1 is the start of P_{CotC} and 2735 is end of CotC. This alignment represents 1832 ~ 2735.

(B)

Figure B.5 Genomic DNA sequencing results of integration of pDG1730 huPTH1R-CotC. **(B)** Genomic DNA sequencing traces were done with the primer seq-huPTH1R CotC-F5. (Continued)

(A)

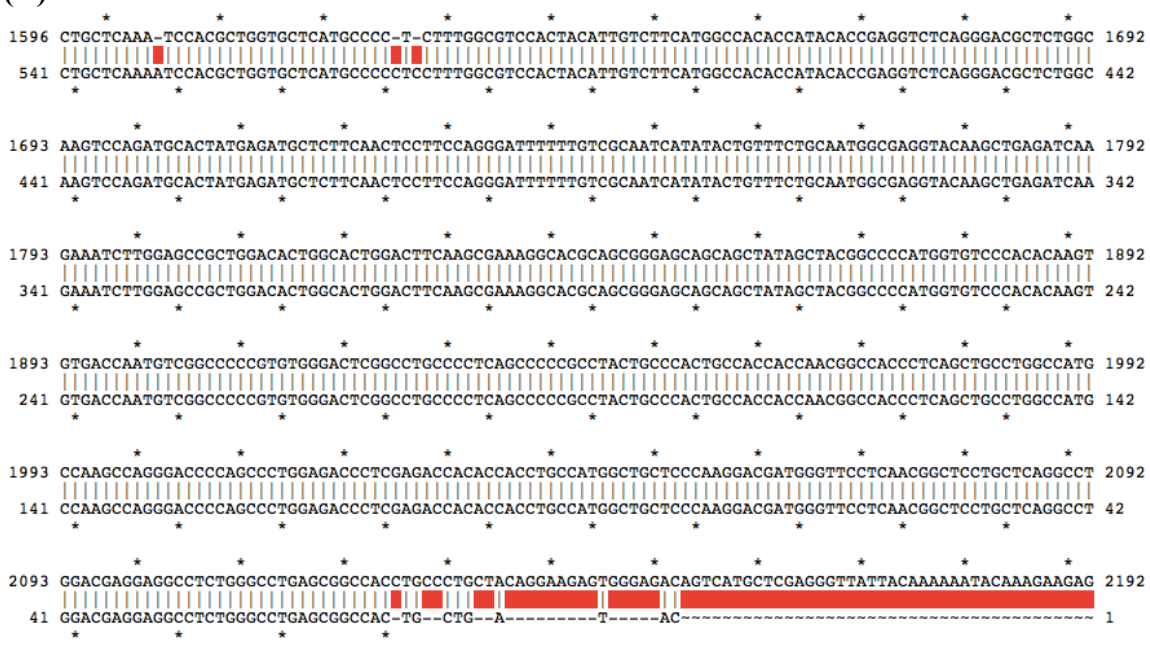

Figure B.6 Genomic DNA sequencing results of integration of pDG1730 huPTH1R-CotC. (A) Top strand is the DNA coding region from the promoter of CotC to CotC, P_{CotC}-huPTH1R-CotC DNA. The bottom strand represents the genomic DNA sequencing results using the primer seq-huPTH1R CotC-R2 (5'-CGGCTCGAGCATGAC TGTCTCCCACTCTTCC-3'). Nucleotide 1 is the start of P_{CotC} and 2735 is end of CotC. This alignment represents 1628 ~ 2124.

(B)

Figure B.6 Genomic DNA sequencing results of integration of pDG1730 huPTH1R-CotC. **(B)** Genomic DNA sequencing traces were done with the primer seq-huPTH1R CotC-R2. (Continued)

(A)

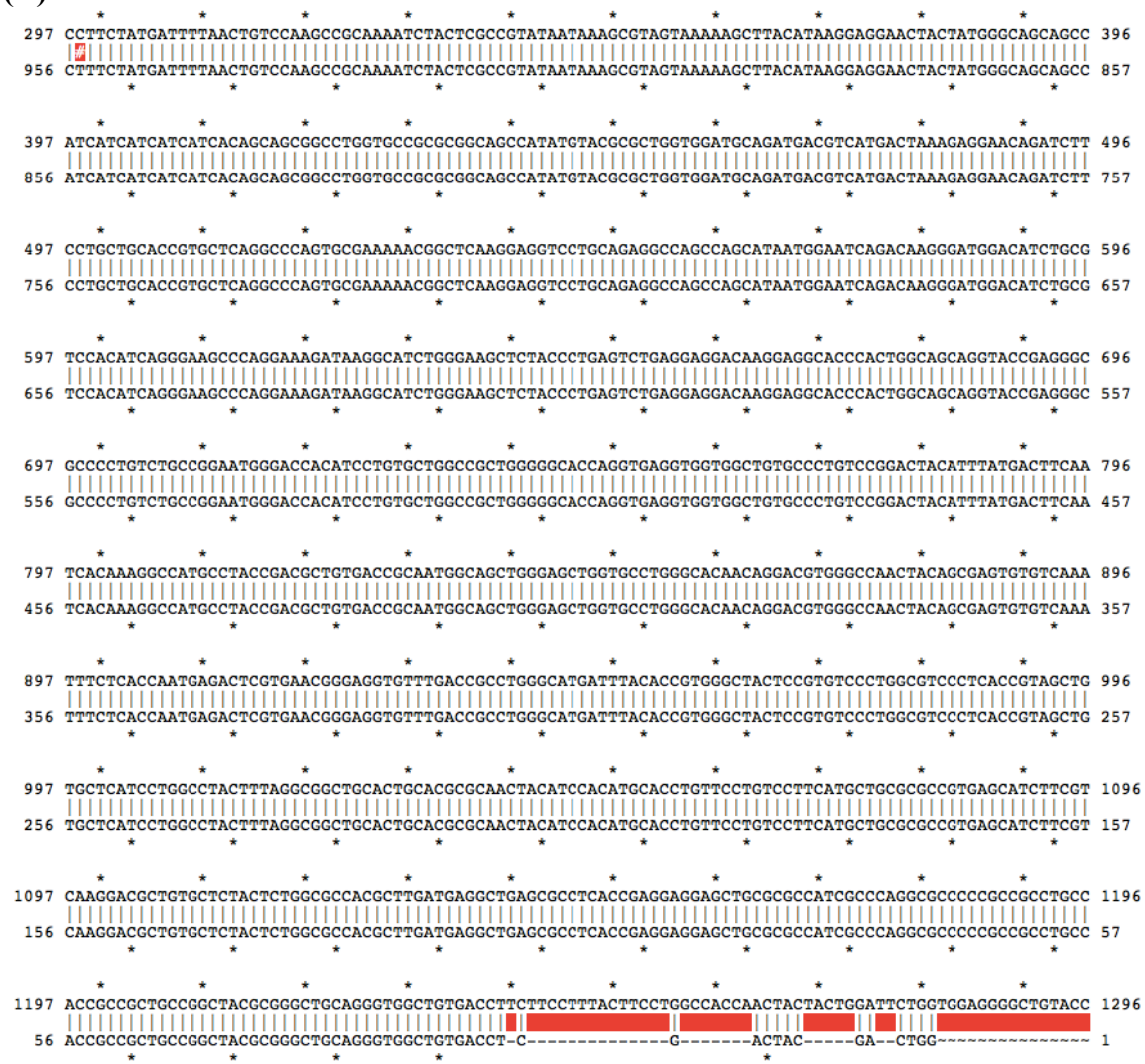

Figure B.7 Genomic DNA sequencing results of integration of pDG1730 huPTH1R-CotC. (A) Top strand is the DNA coding region from the promoter of CotC to CotC, P_{CotC}-huPTH1R-CotC DNA. The bottom strand represents the genomic DNA sequencing results using the primer seq-huPTH1R CotC-R4 (5'-CCAGAATCCAGTAGT AGTTGGTGGCC-3'). Nucleotide 1 is the start of P_{CotC} and 2735 is end of CotC. This alignment represents 300 ~ 1239.

(B)

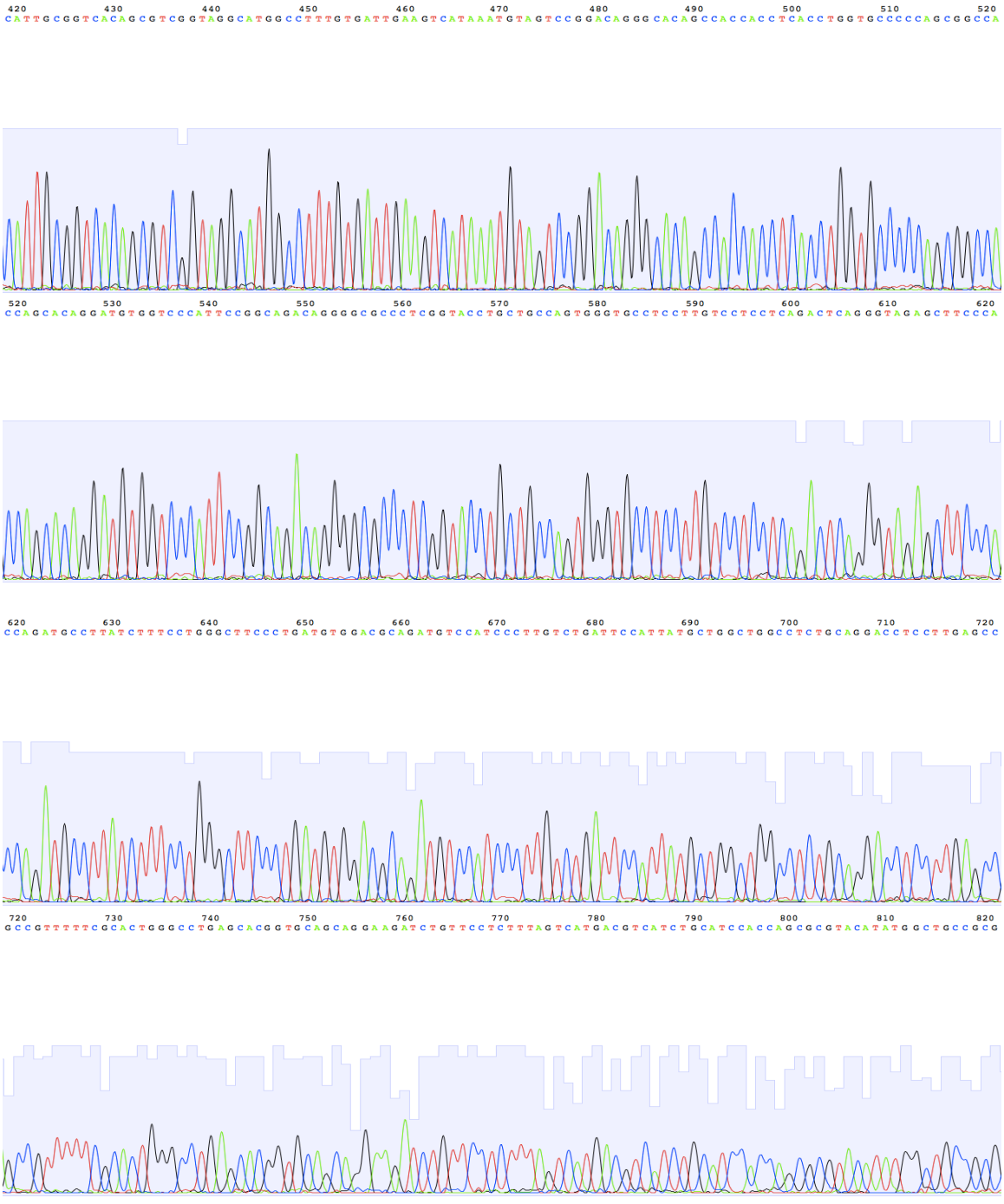

Figure B.7 Genomic DNA sequencing results of integration of pDG1730 huPTH1R-CotC. **(B)** Genomic DNA sequencing traces were done with the primer seq-huPTH1R CotC-R4. (Continued)

(A)

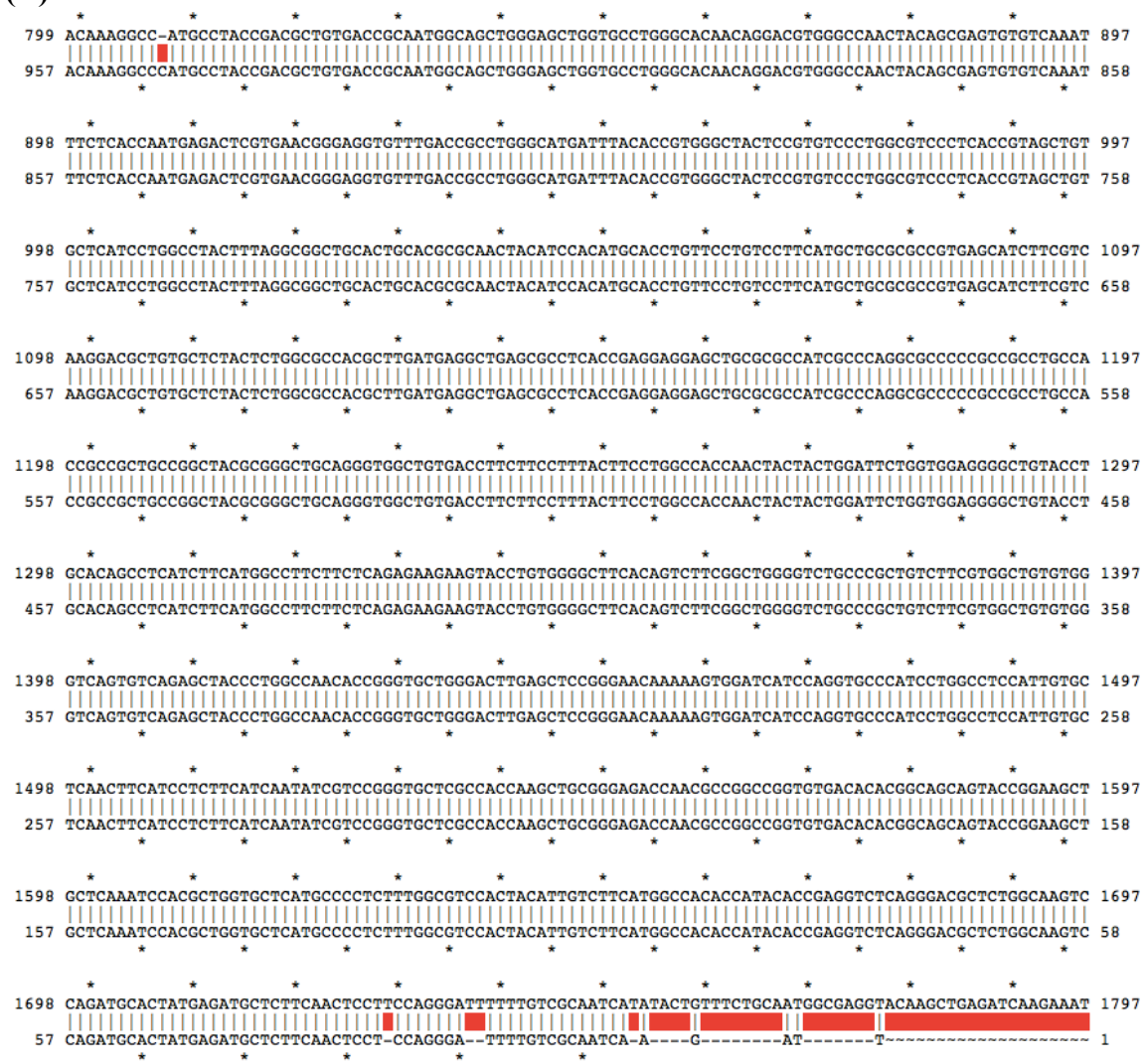

Figure B.8 Genomic DNA sequencing results of integration of pDG1730 huPTH1R-CotC. (A) Top strand is the DNA coding region from the promoter of CotC to CotC, P_{CotC}-huPTH1R-CotC DNA. The bottom strand represents the genomic DNA sequencing results using the primer seq-huPTH1R CotC-R5 (5'-GATCTCAGCTTGTAC CTCGCCATTGC-3'). Nucleotide 1 is the start of P_{CotC} and 2735 is end of CotC. This alignment represents 809 ~ 1729.

(B)

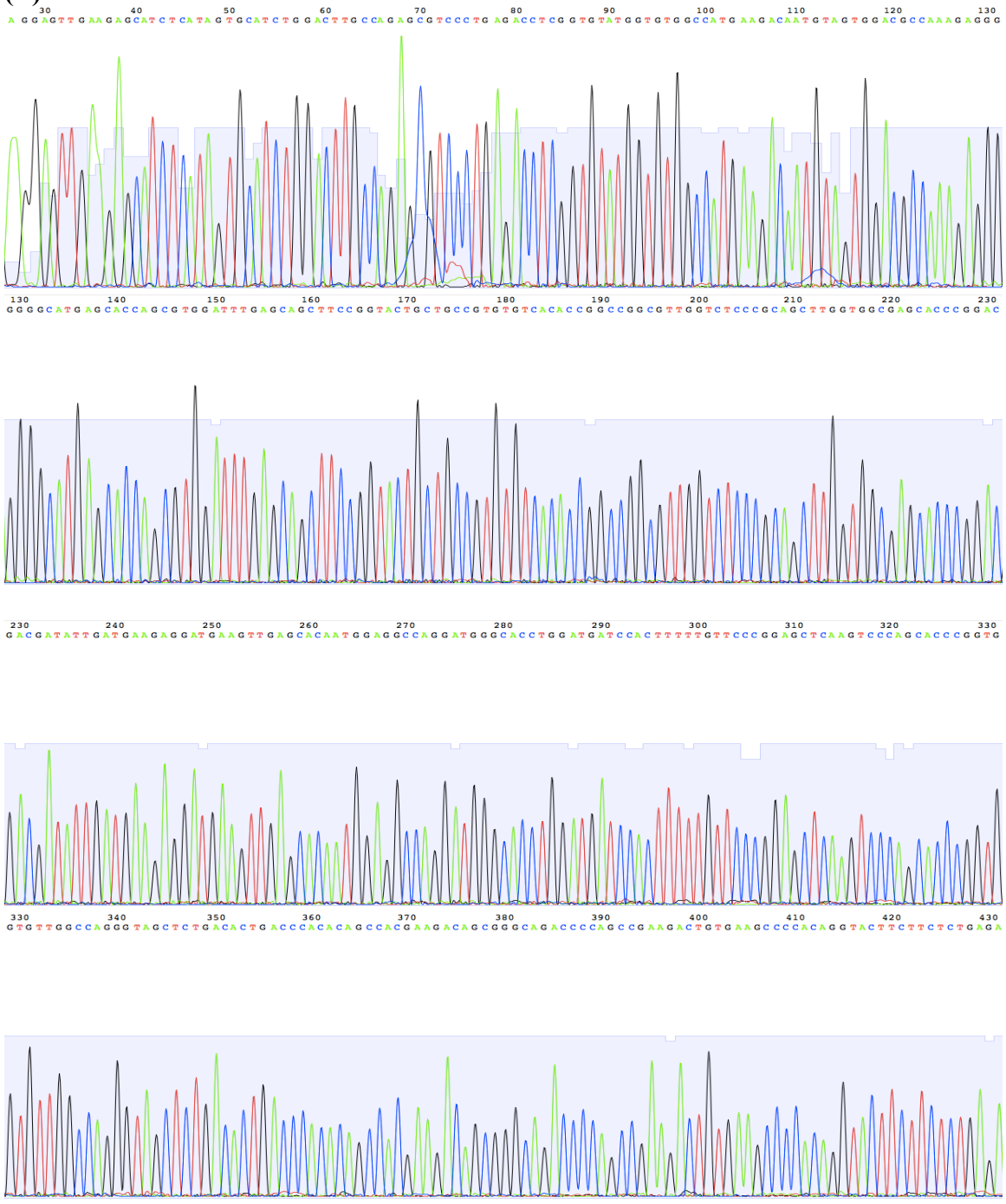
30 40 50 60 70 80 90 100 110 120 130
A G G A G T T G A A G A G C A T C T C A T A G T G C A T C T G G A C T T G C C A G A G C G T C C C T G A G A C C T C G G T G T A T G G T G T G G C C A T G A A G A C A A T G T A G T G G A C G C C A A A G A G G G
130 140 150 160 170 180 190 200 210 220 230
G G G G C A T G A G C A C C A G C G T G G A T T T G A G C A G C T T C C G G T A C T G C T G C C G T G T G T C A C A C C G G C C G G C G T T G G T C T C C C G C A G C T T G G T G G C G A G C A C C C G G A C
230 240 250 260 270 280 290 300 310 320 330
G A C G A T A T T G A T G A A G A G G A T G A A G T T G A G C A C A A T G G A G G C C A G G A T G G G C A C C T G G A T G A T C C A C T T T T T G T T C C C G G A G C T C A A G T C C C A G C A C C C G G T G
330 340 350 360 370 380 390 400 410 420 430
G T G T T G G C C A G G G T A G C T C T G A C A C T G A C C C A C A C A G C C A C G A A G A C A G C G G G C A G A C C C C A G C C G A A G A C T G T G A A G C C C C A C A G G T A C T T C T T C T C T G A G A

Figure B.8 Genomic DNA sequencing results of integration of pDG1730 huPTH1R-CotC. **(B)** Genomic DNA sequencing traces were done with the primer seq-huPTH1R CotC-R5. (Continued)

REFERENCES

1. Abrol, R., and Goddard Iii, F. W. A. (2011) Chapter 11 G Protein-Coupled Receptors: Conformational "Gatekeepers" of Transmembrane Signal Transduction and Diversification, In *Extracellular and Intracellular Signaling*, pp 188-229, The Royal Society of Chemistry.

2. Bockaert, J., and Pin, J. P. (1999) Molecular tinkering of G protein-coupled receptors: An evolutionary success, *EMBO Journal 18*, 1723-1729.

3. Lagerström, M. C., and Schiöth, H. B. (2008) Structural diversity of G protein-coupled receptors and significance for drug discovery, *Nature reviews. Drug discovery 7*, 339-357.

4. Palczewski, K., Kumasaka, T., Hori, T., Behnke, C. A., Motoshima, H., Fox, B. A., Le Trong, I., Teller, D. C., Okada, T., Stenkamp, R. E., Yamamoto, M., and Miyano, M. (2000) Crystal structure of rhodopsin: A G protein-coupled receptor, *Science 289*, 739-745.

5. Murakami, M., and Kouyama, T. (2008) Crystal structure of squid rhodopsin, *Nature 453*, 363-367.

6. Rasmussen, S. G. F., Choi, H. J., Rosenbaum, D. M., Kobilka, T. S., Thian, F. S., Edwards, P. C., Burghammer, M., Ratnala, V. R. P., Sanishvili, R., Fischetti, R. F., Schertler, G. F. X., Weis, W. I., and Kobilka, B. K. (2007) Crystal structure of the human beta 2 adrenergic G-protein-coupled receptor, *Nature 450*, 383-387.

7. Warne, T., Serrano-Vega, M. J., Baker, J. G., Moukhametzianov, R., Edwards, P. C., Henderson, R., Leslie, A. G. W., Tate, C. G., and Schertler, G. F. X. (2008) Structure of a β1-adrenergic G-protein-coupled receptor, *Nature 454*, 486-491.

8. Xu, F., Wu, H., Katritch, V., Han, G. W., Jacobson, K. A., Gao, Z. G., Cherezov, V., and Stevens, R. C. (2011) Structure of an agonist-bound human A 2A adenosine receptor, *Science 332*, 322-327.

9. Shimamura, T., Shiroishi, M., Weyand, S., Tsujimoto, H., Winter, G., Katritch, V., Abagyan, R., Cherezov, V., Liu, W., Han, G. W., Kobayashi, T., Stevens, R. C., and Iwata, S. (2011) Structure of the human histamine H 1 receptor complex with doxepin, *Nature 475*, 65-72.

10. Hanson, M. A., Roth, C. B., Jo, E., Griffith, M. T., Scott, F. L., Reinhart, G., Desale, H., Clemons, B., Cahalan, S. M., Schuerer, S. C., Sanna, M. G., Han, G. W., Kuhn, P., Rosen, H., and Stevens, R. C. (2012) Crystal structure of a lipid G protein-coupled receptor, *Science 335*, 851-855.

11. Wu, B., Chien, E. Y. T., Mol, C. D., Fenalti, G., Liu, W., Katritch, V., Abagyan, R., Brooun, A., Wells, P., Bi, F. C., Hamel, D. J., Kuhn, P., Handel, T. M., Cherezov, V., and Stevens, R. C. (2010) Structures of the CXCR4 chemokine GPCR with small-molecule and cyclic peptide antagonists, *Science 330*, 1066-1071.

12. Rosenbaum, D. M., Rasmussen, S. G. F., and Kobilka, B. K. (2009) The structure and function of G-protein-coupled receptors, *Nature 459*, 356-363.

13. Choe, H. W., Kim, Y. J., Park, J. H., Morizumi, T., Pai, E. F., Krau, N., Hofmann, K. P., Scheerer, P., and Ernst, O. P. (2011) Crystal structure of metarhodopsin II, *Nature 471*, 651-655.

14. Kobilka, B., and Schertler, G. F. X. (2008) New G-protein-coupled receptor crystal structures: insights and limitations, *Trends in Pharmacological Sciences 29*, 79-83.

15. Cherezov, V., Rosenbaum, D. M., Hanson, M. A., Rasmussen, S. G. F., Foon, S. T., Kobilka, T. S., Choi, H. J., Kuhn, P., Weis, W. I., Kobilka, B. K., and Stevens, R. C. (2007) High-resolution crystal structure of an engineered human beta2-adrenergic G protein-coupled receptor, *Science 318*, 1258-1265.

16. Blaber, M., Lindstrom, J. D., Gassner, N., Xu, J., Heinz, D. W., and Matthews, B. W. (1993) Energetic cost and structural consequences of burying a hydroxyl group within the core of a protein determined from Ala ,Üí Ser and Val ,Üí Thr substitutions in T4 lysozyme, *Biochemistry 32*, 11363-11373.

17. Bowler, P. J. (2009) Darwin's Originality, *Science 323*, 223-226.

18. Barlow, M., and Hall, B. G. (2003) Experimental prediction of the natural evolution of antibiotic resistance, *Genetics 163*, 1237-1241.

19. Baqyero, F., and Blázquez, J. (1997) Evolution of antibiotic resistance, *Trends in Ecology and Evolution 12*, 482-487.

20. Wlodawer, A., Borkakoti, N., Moss, D. S., and Howlin, B. (1986) Comparison of two independently refined models of ribonuclease-A, *Acta Crystallographica Section B 42*, 379-387.

21. Leonidas, D. D., Shapiro, R., Allen, S. C., Subbarao, G. V., Veluraja, K., and Acharya, K. R. (1999) Refined crystal structures of native human angiogenin and two active site variants: Implications for the unique functional properties of an enzyme involved in neovascularisation during tumour growth, *Journal of Molecular Biology 285*, 1209-1233.

22. Hutchison Iii, C. A., Phillips, S., and Edgell, M. H. (1978) Mutagenesis at a specific position in a DNA sequence, *Journal of Biological Chemistry 253*, 6551-6560.

23. Declerck, N., Machius, M., Wiegand, G., Huber, R., and Gaillardin, C. (2000) Probing structural determinants specifying high thermostability in Bacillus licheniformis α-amylase, *Journal of Molecular Biology 301*, 1041-1057.

24. Igarashi, K., Ozawa, T., Ikawa-Kitayama, K., Hayashi, Y., Araki, H., Endo, K., Hagihara, H., Ozaki, K., Kawai, S., and Ito, S. (1999) Thermostabilization by proline substitution in an alkaline, liquefying α-amylase from Bacillus sp. strain KSM-1378, *Bioscience, Biotechnology and Biochemistry 63*, 1535-1540.

25. Zhu, G. P., Xu, C., Teng, M. K., Tao, L. M., Zhu, X. Y., Wu, C. J., Hang, J., Niu, L. W., and Wang, Y. Z. (1999) Increasing the thermostability of D-xylose isomerase by introduction of a proline into the turn of a random coil, *Protein Engineering 12*, 635-638.

26. Ueda, T., Masumoto, K., Ishibashi, R., So, T., and Imoto, T. (2000) Remarkable thermal stability of doubly intramolecularly cross-linked hen lysozyme, *Protein Engineering 13*, 193-196.

27. Asano, Y., Kira, I., and Yokozeki, K. (2005) Alteration of substrate specificity of aspartase by directed evolution, *Biomolecular Engineering 22*, 95-101.

28. Bornscheuer, U. T., and Pohl, M. (2001) Improved biocatalysts by directed evolution and rational protein design, *Current Opinion in Chemical Biology 5*, 137-143.

29. Kaur, J., and Sharma, R. (2006) Directed evolution: An approach to engineer enzymes, *Critical Reviews in Biotechnology 26*, 165-199.

30. Farinas, E. T., Bulter, T., and Arnold, F. H. (2001) Directed enzyme evolution, *Current Opinion in Biotechnology 12*, 545-551.

31. Eijsink, V. G. H., GÅseidnes, S., Borchert, T. V., and Van Den Burg, B. (2005) Directed evolution of enzyme stability, *Biomolecular Engineering 22*, 21-30.

32. Hida, K., Hanes, J., and Ostermeier, M. (2007) Directed evolution for drug and nucleic acid delivery, *Advanced Drug Delivery Reviews 59*, 1562-1578.

33. Samuelson, P., Gunneriusson, E., Nygren, P. Å., and Ståhl, S. (2002) Display of proteins on bacteria, *Journal of Biotechnology 96*, 129-154.

34. Lee, S. Y., Choi, J. H., and Xu, Z. (2003) Microbial cell-surface display, *Trends in Biotechnology 21*, 45-52.

35. Li, M. (2000) Applications of display technology protein analysis, *Nature Biotechnology 18*, 1251-1256.

36. Kim, J., and Schumann, W. (2009) Display of proteins on bacillus subtilis endospores, *Cellular and Molecular Life Sciences 66*, 3127-3136.

37. Benhar, I. (2001) Biotechnological applications of phage and cell display, *Biotechnology Advances 19*, 1-33.

38. Efimov, V. P., Nepluev, I. V., and Mesyanzhinov, V. V. (1995) Bacteriophage T4 as a surface display vector, *Virus Genes 10*, 173-177.

39. Bratkovič, T. (2010) Progress in phage display: Evolution of the technique and its applications, *Cellular and Molecular Life Sciences 67*, 749-767.

40. Smith, G. P., and Petrenko, V. A. (1997) Phage Display, *Chemical Reviews 97*, 391-410.

41. Pepper, L. R., Yong, K. C., Boder, E. T., and Shusta, E. V. (2008) A decade of yeast surface display technology: Where are we now?, *Combinatorial Chemistry and High Throughput Screening 11*, 127-134.

42. Smith, G. P. (1985) Filamentous fusion phage: Novel expression vectors that display cloned antigens on the virion surface, *Science 228*, 1315-1317.

43. Kehoe, J. W., and Kay, B. K. (2005) Filamentous phage display in the new millennium, *Chemical Reviews 105*, 4056-4072.

44. Castagnoli, L., Zucconi, A., Quondam, M., Rossi, M., Vaccaro, P., Panni, S., Paoluzi, S., Santonico, E., Dente, L., and Cesareni, G. (2001) Alternative bacteriophage display systems, *Combinatorial Chemistry and High Throughput Screening 4*, 121-133.

45. Ren, Z. J., Lewis, G. K., Wingfield, P. T., Locke, E. G., Steven, A. C., and Black, L. W. (1996) Phage display of intact domains at high copy number: A system based on SOC, the small outer capsid protein of bacteriophage T4, *Protein Science 5*, 1833-1843.

46. Santini, C., Brennan, D., Mennuni, C., Hoess, R. H., Nicosia, A., Cortese, R., and Luzzago, A. (1998) Efficient display of an HCV cDNA expression library as C-terminal fusion to the capsid protein D of bacteriophage lambda, *Journal of Molecular Biology 282*, 125-135.

47. Sheets, M. D., Amersdorfer, P., Finnern, R., Sargent, P., Lindqvist, E., Schier, R., Hemingsen, G., Wong, C., Gerhart, J. C., and Marks, J. D. (1998) Efficient construction of a large nonimmune phage antibody library: The production of high-affinity human single-chain antibodies to protein antigens, *Proceedings of the National Academy of Sciences of the United States of America 95*, 6157-6162.

48. De Haard, H. J., Van Neer, N., Reurs, A., Hufton, S. E., Roovers, R. C., Henderikx, P., De Bruïne, A. P., Arends, J. W., and Hoogenboom, H. R. (1999) A large non-immunized human Fab fragment phage library that permits rapid isolation and kinetic analysis of high affinity antibodies, *Journal of Biological Chemistry 274*, 18218-18230.

49. Heyd, B., Pecorari, F., Collinet, B., Adjadj, E., Desmadril, M., and Minard, P. (2003) In vitro evolution of the binding specificity of neocarzinostatin, an enediyne-binding chromoprotein, *Biochemistry 42*, 5674-5683.

50. Sarikaya, M., Tamerler, C., Jen, A. K. Y., Schulten, K., and Baneyx, F. (2003) Molecular biomimetics: Nanotechnology through biology, *Nature Materials 2*, 577-585.

51. Kristensen, P., and Winter, G. (1998) Proteolytic selection for protein folding using filamentous bacteriophages, *Folding and Design 3*, 321-328.

52. Sieber, V., Plückthun, A., and Schmid, F. X. (1998) Selecting proteins with improved stability by a phage-based method, *Nature Biotechnology 16*, 955-960.

53. Chen, W., and Georgiou, G. (2002) Cell-surface display of heterologous proteins: From high-throughput screening to environmental applications, *Biotechnology and Bioengineering 79*, 496-503.

54. Gai, S. A., and Wittrup, K. D. (2007) Yeast surface display for protein engineering and characterization, *Current Opinion in Structural Biology 17*, 467-473.

55. Boder, E. T., and Wittrup, K. D. (1997) Yeast surface display for screening combinatorial polypeptide libraries, *Nature Biotechnology 15*, 553-557.

56. Shibasaki, S., Ueda, M., Ye, K., Shimizu, K., Kamasawa, N., Osumi, M., and Tanaka, A. (2001) Creation of cell surface-engineered yeast that display different fluorescent proteins in response to the glucose concentration, *Applied Microbiology and Biotechnology 57*, 528-533.

57. Schreuder, M. P., Deen, C., Boersma, W. J. A., Pouwels, P. H., and Klis, F. M. (1996) Yeast expressing hepatitis B virus surface antigen determinants on its surface: Implications for a possible oral vaccine, *Vaccine 14*, 383-388.

58. Leemhuis, H., Stein, V., Griffiths, A. D., and Hollfelder, F. (2005) New genotype-phenotype linkages for directed evolution of functional proteins, *Current Opinion in Structural Biology 15*, 472-478.

59. Hoogenboom, H. R. (2005) Selecting and screening recombinant antibody libraries, *Nature Biotechnology 23*, 1105-1116.

60. Lamla, T., and Erdmann, V. A. (2003) Searching sequence space for high-affinity binding peptides using ribosome display, *Journal of Molecular Biology 329*, 381-388.

61. Jermutus, L., Honegger, A., Schwesinger, F., Hanes, J., and Plückthun, A. (2001) Tailoring in vitro evolution for protein affinity or stability, *Proceedings of the National Academy of Sciences of the United States of America 98*, 75-80.

62. Lipovsek, D., and Plückthun, A. (2004) In-vitro protein evolution by ribosome display and mRNA display, *Journal of Immunological Methods 290*, 51-67.

63. Cujec, T. P., Medeiros, P. F., Hammond, P., Rise, C., and Kreider, B. L. (2002) Selection of v-abl tyrosine kinase substrate sequences from randomized peptide and cellular proteomic libraries using mRNA display, *Chemistry and Biology 9*, 253-264.

64. Hammond, P. W., Alpin, J., Rise, C. E., Wright, M., and Kreider, B. L. (2001) In Vitro Selection and Characterization of Bcl-XL-binding Proteins from a Mix of Tissue-specific mRNA Display Libraries, *Journal of Biological Chemistry 276*, 20898-20906.

65. Losick, R., Youngman, P., and Piggot, P. J. (1986) Genetics of endospore formation in Bacillus subtilis, *Annual Review of Genetics 20*, 625-669.

66. Bornscheuer, U. T. (2003) Immobilizing enzymes: How to create more suitable biocatalysts, *Angewandte Chemie - International Edition 42*, 3336-3337.

67. Gupta, N., and Farinas, E. T. (2010) Directed evolution of CotA laccase for increased substrate specificity using Bacillus subtilis spores, *Protein Engineering, Design and Selection 23*, 679-682.

68. Michalke, K., Huyghe, C., Lichière, J., Gravière, M. E., Siponen, M., Sciara, G., Lepaul, I., Wagner, R., Magg, C., Rudolph, R., Cambillau, C., and Desmyter, A. (2010) Mammalian G protein-coupled receptor expression in Escherichia coli: II. Refolding and biophysical characterization of mouse cannabinoid receptor 1 and human parathyroid hormone receptor 1, *Analytical Biochemistry 401*, 74-80.

69. Sarkar, C. A., Dodevski, I., Kenig, M., Dudli, S., Mohr, A., Hermans, E., and Plückthun, A. (2008) Directed evolution of a G protein-coupled receptor for expression, stability, and binding selectivity, *Proceedings of the National Academy of Sciences of the United States of America 105*, 14808-14813.

70. Gardella, T. J., and Jüppner, H. (2001) Molecular properties of the PTH/PTHrP receptor, *Trends in Endocrinology and Metabolism 12*, 210-217.